Scientific Report No. 38

A UNIFIED THEORY FOR THIN WIRE ANTENNAS OF ARBITRARY LENGTH

by

Larry Rispin and David C. Chang

Electromagnetics Laboratory
Department of Electrical Engineering
University of Colorado
Boulder, Colorado 80309

February 1980

Prepared for

US Office of Naval Research
Arlington, Virginia 22217

This project is monitored by Dr. H. Mullaney of the Office of Naval Research under contract no. N0014-76-C-0318.

ABSTRACT

A simple theory based upon traveling wave concepts and the Wiener-Hopf technique is developed which describes the current distributions on tubular cylindrical receiving and transmitting antennas. A close examination of the conditions necessary to obtain sufficiently accurate asymptotic solutions for reflected current distributions is given along with several numerical examples for cooboration. This along with corresponding modifications to other relevant terms in the traveling wave solution for a finite length cylindrical antenna allow for the consideration of a much wider range of cylindrical antennas than normally possible under the traditional thin-wire approximations, $ka \ll 1$ and $kh \gtrsim 1$. Specific examples discussed include electrically short, ($kh = 0.4$ and $\Omega(h) = 2\,\ell n(2h/a) = 10$), practical half-wave, ($kh = \pi/2$ and $\Omega(h) = 2\,\ell n(2h/a) = 10$), and electrical thick, ($ka = 1$ and $kh = 3\pi$), receiving and transmitting antennas. Comparisons with existing theories in these cases and others yield very acceptable agreements. Further, the receiving antenna formulation allows for an arbitrary angle of incidence, $0 \leq \theta_i \leq \pi$, of the uniform plane wave and the transmitting antenna formulation gives excellent input conductance data over an extremely wide range of antenna parameters. Discussions are given for such related topics as the current distributions on the internal wall of a cylindrical antenna, loaded cylindrical antennas and the far field radiation pattern of a cylindrical transmitting antenna.

Table of Contents

1. Introduction

As is well known, thin-wire conductors are commonly used as radiators in the design of antenna systems. The radius, a, of each wire is typically much smaller than its half length, h, which for most applications is of the order of a wavelength, λ. Only in limited situations, such as the case of probing an unknown field, will the length be much smaller than a free-space wavelength, (i.e., $2h << \lambda$), or as in the case of a trailing antenna behind an aircraft, will the length be much greater than a free space wavelength, (i.e., $2h >> \lambda$). Consequently most linear antenna theories, both analytical and numerical, are developed with an explicit or implicit assumption that $a << \lambda$ and $2h \gtrsim \lambda/2$, which is commonly referred to as the thin wire assumption. On the other hand, theories not in this general category, usually have a much more limited range of application, such as for the very short antenna and the very long antenna.

More recently, the time-transient response, as well as the broadband frequency response of a thin-wire structure has become a problem of considerable importance. For instance, in order to access the susceptibility of a long thin cylindrical metallic enclosure, one must obtain statistical information concerning the performance of the cylinder as a receiving antenna, over an extremely wide frequency range as well as an arbitrary angle of incidence (referring to illumination by an incident plane wave). Computations not only become excessive when conventional theories are utilized because virtually thousands of responses are needed, but also very awkward since different methods have to be used in different frequency ranges. A similar statement, of course, can also be made for studying the impulse response of an antenna.

Beginning with Hallén's [1] integral equation formulation for the current on a cylindrical antenna and including the work of many others [2] - [10], the thin-wire approximations mentioned above have nearly always been employed. Weinstein [2] did, however, observe that his final approximate solutions, which were derived under the thin wire assumptions, could be applied to cylinders having larger values of ka if the electrical length, kz, were very much larger. In contrast, the theory of King and Middleton [11, Chap. II], however, which involves the iterative solution of an integral equation for the current on a finite length cylinder, requires explicitly that the parameter, $\Omega = 2\,\ell n(2h/a)$, to be large, h being the half-length of the cylinder. Although the parameter, Ω, relates only to the physical length and radius of the antenna, this approach still requires the electrical radius, ka, to be small compared to unity and the electrical length, kh, cannot be very small nor very large. King also developed a receiving theory [11, Chap. IV] for antennas having a large Ω. A large Ω was also the basis for two electrically short ($kh \lesssim 1$) antenna theories developed by King [11, Sec.II.31 and IV.8] and [12, Sec. 3.7] which were developed by making approximations relevant to the short antenna situation in the integral equation formulation of the problem.

Another means of analysis for the cylindrical antenna problem is the numerical method of moments technique [13], which has the capability of computing antenna characteristics without invoking the thin wire approximations. Realistically, however, the computation time is considerable if the antenna is not thin or the length is more than a few free space wavelengths.

In this paper, our aim is to develop a simple unified theory for computing the broadband characteristics of a transmitting and/or receiving antenna when the parameter, $\Omega = 2\ \ell n(2h/a)$ is large. For a typical thin-wire antenna where $\Omega = 2\ \ell n(2h/a) = 10$, our theory is applicable for antenna lengths as short as $2h \approx 0.12\lambda$ and as long as $2h \approx 23\lambda$ (where for $\Omega = 10$, ka is almost equal to 1), which in terms of frequency covers well over two orders of magnitude and is more than adequate even for transient computations. We also show that our formulation may be applied to an electrically thick (up to $ka = 1$) cylindrical transmitting antenna or the electrically thick receiving antenna (for the angularly independent current) and obtain favorable agreement with existing theories even when the parameter $\Omega = 2\ \ell n(2h/a)$ is not large.

We begin with a re-examination of the conditions necessary to obtain simple approximate solutions to cylindrical antenna problems via the Wiener-Hopf technique. Section 2 discusses a pair of canonical integrals which characterize cylindrical antenna problems. Approximate expressions for these canonical integrals are derived subject to the condition, $\Omega(z) = 2\ \ell n(2z/a) >> |\ell n[2kz\ \sin^2(\theta_i/2)]|$. The angle, θ_i, refers to the incident angle of the incoming wave and is more fully described later. In Section 3 the various currents on both infinite and semi-infinite cylindrical receiving and transmitting antennas are given and their relationships to the canonical integrals established. Data obtained from the approximate expressions is then compared with numerically evaluated "exact" data in Section 4. A most important observation in this section is that the parameter, $\Omega(z) = 2\ \ell n(2z/a)$, in the basic condition of our analysis, need not be very much larger than $|\ell n[2kz\ \sin^2(\theta_i/z)]|$, especially when thicker antennas $(ka \gtrsim 0.1)$

are involved. Utilizing the process of summing multiple reflections, approximate expressions for the receiving and transmitting currents and the input admittance for finite length cylindrical antennas are formulated in Section 5. Expressions for the currents flowing on the internal walls of receiving and transmitting tubular antennas are given in Section 6. In Section 7, numerical results from our theory for specific antennas are compared with the results of other authors using different approaches, with acceptable agreement in all the cases considered. The special case of the electrically short antenna is discussed in Section 8. General conclusions as well as extensions of our theory to loaded antennas and the determination of the far field radiation from a transmitting antenna are given in Section 9.

The exact integral expressions appearing in Section 4 are for the most part, based upon the Wiener-Hopf technique (see for example Nobel [14], Weinstein [2] and Mittra and Lee [15]). The assumed time variation is $e^{-i\omega t}$ and the implied Fourier transform pair is given by,

$$\tilde{F}(\alpha) = \int_{-\infty}^{\infty} F(z) e^{i\alpha z}\, dz \tag{1}$$

and

$$F(z) = \frac{1}{2\pi} \int_{-\infty}^{\infty} \tilde{F}(\alpha) e^{-i\alpha z}\, d\alpha \ . \tag{2}$$

2. The canonical integral in cylindrical antenna problems

As will be shown later, the external current distributions on both the receiving and transmitting cylindrical antennas can be written in terms of the canonical integral,

$$U(\theta_i;z) = -i\frac{k}{\eta}(1 - \cos\theta_i)\int_{\Gamma_0}\frac{e^{-i\alpha z}}{(k+\alpha)(k\cos\theta_i+\alpha)K(\alpha)}\,d\alpha$$

$$; 0 \le z < \infty,\ 0 \le \theta_i \le \pi \qquad (3)$$

The contour, Γ_0, is shown in Figure 1 and,

$$K(\alpha) = i\pi J_0(\xi a)\,H_0^{(1)}(\xi a) \qquad (4)$$

where

$$\xi = \sqrt{k^2 - \alpha^2} = i\sqrt{\alpha^2 - k^2}$$

θ_i is the incident angle of the incoming current wave when (3) is used to describe a particular current distribution reflected from an end of a cylinder and z is a numerical distance along the axis of the antenna. $k = 2\pi/\lambda$ and η are the plane wave wavenumber and the intrinsic impedance, respectively, of the medium surrounding the antenna. The antenna to be considered is assumed to have an infinitely-thin, perfectly-conducting wall concentric about the z-axis at a radius, a. The suppressed time factor is $\exp(-i\omega t)$, where ω is the operating frequency in radians/sec.

We shall also find it useful to define the auxiliary canonical integral, $W(\theta_i;z)$, which is similar to $U(\theta_i;z)$ in (3) except for the appearance in the integrand of the additional function, $K_+(\alpha)$, defined as the factor of $K(\alpha)$ in (4) which is analytic and free of zeroes in the upper half complex α-plane,

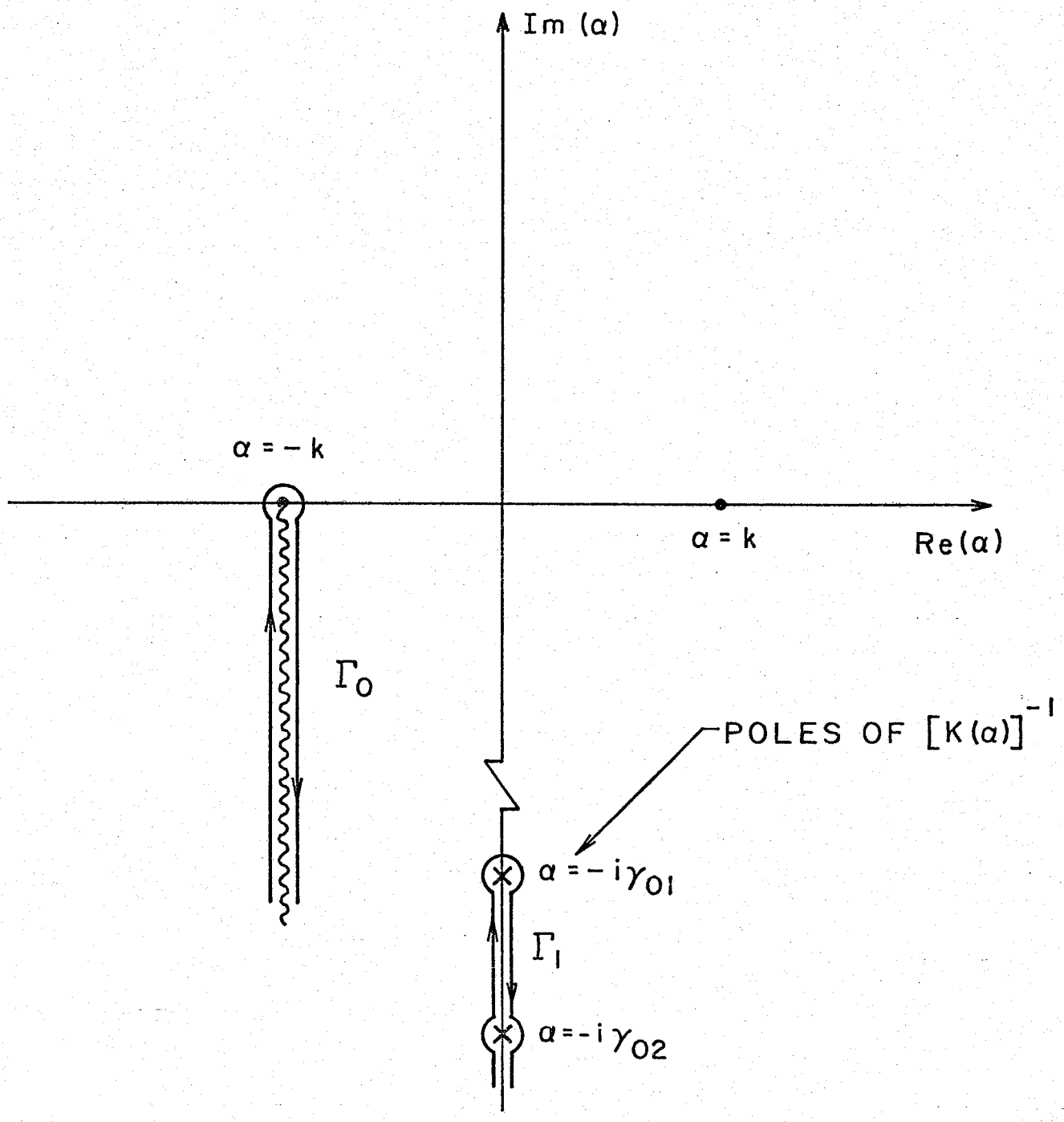

Figure 1. The complex α-plane

$$W(\theta_i;z) = -i\,\frac{k}{\eta}\,(1 - \cos\,\theta_i)\int_{\Gamma_0} \frac{K_+(-\alpha)e^{-i\alpha z}}{(k+\alpha)(k\,\cos\,\theta_i+\alpha)\,K(\alpha)}\,d\alpha$$

$$; \; 0 \le z \le \infty, \; 0 \le \theta_i \le \pi \tag{6}$$

Properties of $K_+(\alpha)$ are discussed in Appendix C. We note that the integral $W(\theta_i;z)$ usually occurs in problems concerning the currents reflected from the ends of cylindrical antennas. As shown in (A8) of Appendix A, when $z >> a$, we may approximate (6) by

$$W(\theta_i;z) \approx K_+(k)U(\theta_i;z) \tag{7}$$

where $U(\theta_i;z)$ is our original canonical integral given in (3). Thus with $W(\theta_i;z)$ given in terms of $U(\theta_i;z)$, our particular use of the form of $W(\theta_i;z)$ in (6) will be limited to providing exact date (from the numerical integration of (6)) to compare with the approximate solutions to follow.

Subject to the condition,

$$\Omega(z) = 2\,\ell n\left(\frac{2z}{a}\right) >> \left|\ell n\left[2kz\,\sin^2\left(\frac{\theta_i}{2}\right)\right]\right| \tag{8}$$

an approximate solution to the canonical integral, $U(\theta_i;z)$, is obtained to order $[\Omega(z)]^{-2}$ in Appendix A. From (A17) of Appendix A, this approximate solution may be stated as

$$U(\theta_i;z) = \frac{i}{\eta}\,e^{ikz}\{\ell n[f(\theta_i;z) - i\pi] - \ell n[f(\theta_i;z) + i\pi]\} \tag{9}$$

where

$$f(\theta_i;z) = 2C_w + \gamma + i\pi/2 + \ell n(2kz) + e^{-iv_0}\,E_1(-iv_0) \tag{10}$$

is a slowly varying function of z . C_w is defined as

$$C_w = - \ell n(ka) - \gamma \quad ; \gamma = 0.57721..... \tag{11}$$

which is usually taken as a large parameter in the typical thin wire application and,

$$v_0 = v_0(\theta_i, z) = 2\ kz\ \sin^2\left(\frac{\theta_i}{2}\right) \tag{12}$$

The function, E_1, appearing in (10) is the exponential integral of the first kind defined in Equation 5.1.1 of [16]. We note that the antenna parameter, $\Omega(z)$, is defined in the same way as in [11] where it has been used as a large parameter for the iterative solution of the antenna problem.

Another approximate form of the canonical integral, $U(\theta_i;z)$, which stems from a Taylor series expansion of (9) subject to the basic restriction stated in (8) is given in (A18) of Appendix A and repeated here,

$$U(\theta_i;z) = \frac{2\pi}{\eta}\,\frac{e^{ikz}}{f(\theta_i;z)} \tag{13}$$

Even though (9) and (13) are equivalent with respect to the order of approximation (i.e., $[\Omega(z)]^{-2}$), we shall find (13) to have a more desirable behavior in the near-grazing, $\theta_i \sim 0$, and near the end, $z \sim 0$, situations. Otherwise, (9) will appear to be a more accurate result than is (13) for $U(\theta_i;z)$.

It is interesting to compare our approximate forms of $U(\theta_i;z)$ to similar expressions derived by other authors. For the current on an infinitely long transmitting antenna ($\theta_i = \pi$), Shen, Wu and King [6] by a semi-

analytical, semi-curve fitting technique found a result similar to our $U(\theta;z)$ in (9), except that the term, $\ell n[kz + \sqrt{(kz)^2 + \exp(-2\gamma)}$, replaces our terms, $\ell n(2kz) + \exp(-i2kz)E_1(-i2kz)$. Thus for large kz, our approximate solution for $U(\pi;z)$ in (9) and that of Shen, et al. [6, Eq. 6] are quite similar. Weinstein [2] found an approximate solution to an integral similar to (3), (he called it the "key" integral), but having a different coefficient outside the integral. Apart from this coefficient (our approach introduces this term at a later time), Weinstein obtained, through a complicated variational approach, an approximate result equivalent to our second approximate form of $U(\theta_i;z)$ in (13). Also, in a more recent work by Chang, Lee and Rispin [17], a further approximation of (13) was obtained and used in a receiving antenna analysis. However, the analyses of Shen,et al., Weinstein and Chang, et al., mentioned above, all assumed the conventional thin wire restrictions,

$$ka << 1 \quad (\text{and} \quad kz > 1) \tag{14}$$

Although in [2], Weinstein did observe, a posteriori,that the approximate form of his "key" integral (similar to (13)) could be used for larger values of ka if at the same time, kz was very much larger. Thus, the importance of our work is not so much contained in the approximate formulas for $U(\theta_i;z)$ in (9) and (13), but rather in the realization of a less restrictive condition (given in (8)) for the validity of these approximate formulas. In fact, it will be shown in Section 4 that the approximate formulas for $U(\theta_i;z)$ in (9) and (13) yield remarkably good agreement with numerically obtained "exact" results even when $\Omega(z)$ is of the same order as $|\ell n(v_0)|$. Hence, even the "much greater" restriction appearing in (8) can be significantly relaxed.

3. Currents on cylindrical antennas

In this section, the currents on infinite and semi-infinite cylindrical receiving and transmitting antennas, given in terms of the canonical integral, $U(\theta_i;z)$ in (3) of Section 2, are described.

3.1 Primary receiving current

The longitudinal current averaged over the circumference on an infinitely long cylindrical antenna due to a plane wave polarized in the same plane as the antenna and incident at an angle, θ_i, with respect to the cylinder axis (which is also the z-axis as shown in Figure 2a), may be written as [8, eq. 10],

$$I_{\infty}^{R}(\theta_i,z) = E_{\theta}^{i}\, V(\theta_i;z) \tag{15}$$

where,

$$V(\theta_i;z) = -i\,\frac{4\pi}{k\eta}\,\frac{J_0(ka\sin\theta_i)}{\sin\theta_i\, K(k\cos\theta_i)}\, e^{ikz\cos\theta_i}\ ;\ -\infty < z < \infty\ ,$$

$$0 \le \theta_i \le \pi \tag{16}$$

J_0 is the zero order Bessel function and $K(\alpha)$ is given in (4). $k = 2\pi/\lambda$ and η are the plane wave propagation constant and intrinsic impedance, respectively, of the surrounding medium. Higher order variations of the z-directed current with respect to the azimuthal angle, ϕ, and the ϕ-directed currents on the cylinder are not treated in this report. Thus, while $V(\theta_i;z)$ represents the total longitudinal current on an infinitely long electrically thin ($ka \ll 1$) antenna very well, it corresponds only to the azimuthally uniform longitudinally directed current on an infinite cylindrical antenna in general.

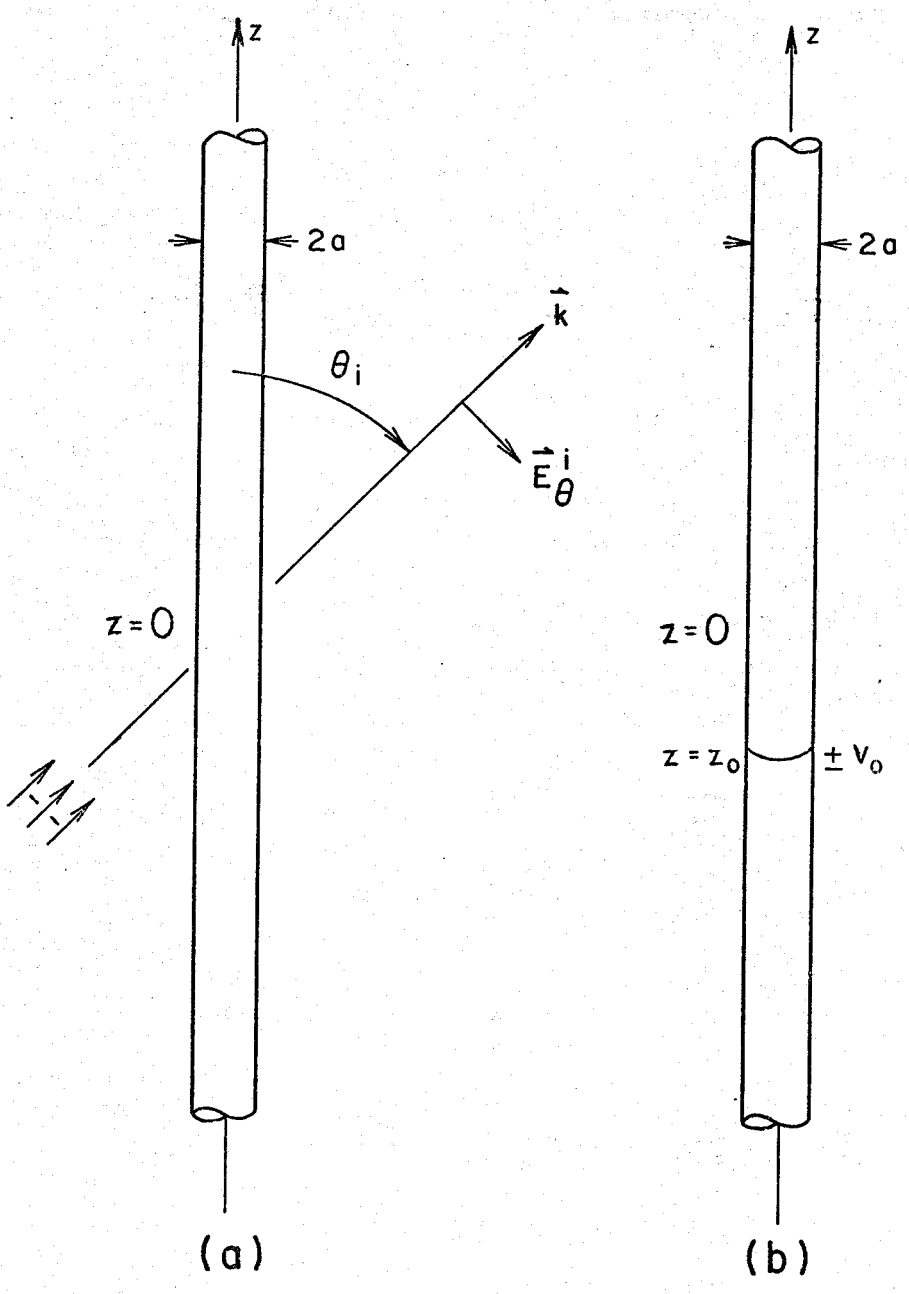

Figure 2. Infinitely long tubular cylindrical antennas

a. receiving; uniform plane wave incident at an angle, θ_i, with respect to the z (antenna) axis.

b. transmitting; delta function voltage source of strength, V_0 volts, located at $z = z_0$.

In the special case of a thin cylinder, i.e., ka << 1, the Bessel function and kernel, $K(\alpha)$ in (4), may be approximated by the leading terms in their respective small argument expressions to yield,

$$V(\theta_i;z) = -i\,\frac{4\pi}{k\eta}\,\frac{e^{ikz\cos\theta_i}}{\sin\theta_i\left[2C_w + i\pi - 2\,\ell n\left(\frac{\sin\theta_i}{2}\right)\right]}\;;\; ka << 1 \qquad (17)$$

where C_w is given in (11).

3.2 Primary transmitting current

The longitudinal current on an infinitely long hollow cylinder due to a uniform (with respect to the azimuthal angle, ϕ) delta function voltage source of strength, V_0, at $z = z_0$ (see Figure 2b), may be written as [6, Eq. 1],

$$I_\infty^T(z_0;z) = i\,\frac{2k}{\eta}\,V_0\int_{\Gamma_0}\frac{e^{-i\alpha|z-z_0|}}{(k^2-\alpha^2)K(\alpha)}\,d\alpha\;;\quad -\infty < z < \infty \qquad (18)$$

where the contour, Γ_0, is shown in Figure 1 and $K(\alpha)$ is given in (4). Comparing (18) with the canonical integral definition in (3), we may write the driven infinite cylinder current as

$$I_\infty(z_0;z) = V_0 U(\pi;|z-z_0|)\;;\; -\infty < z < \infty \qquad (19)$$

and use either approximate form of $U(\pi,z)$ in (9) or (13) to determine this current provided the restriction in (8) is satisfied. This procedure, however, does not yield a good result at the source since the condition on $\Omega(z)$ is violated. In particular, the real part of the current at the source needs to be evaluated very accurately, since physically it

corresponds to the input conductance and hence the power that can be radiated from the antenna. To this end, it is shown in Appendix B, how an approximate expression for primary transmitting current similar to that of Shen, et al. [6] may be constructed. This current expression denoted as $U_s(|z-z_0|)$ replaces the term $U(\pi;|z-z_0|)$ in (19) and is given by

$$U_s(|z-z_0|) = \frac{i}{\eta} e^{ik|z-z_0|} \{\ell n[f_s(|z-z_0|) - i\pi] - \ell n[f_s(|z-z_0|) + i\pi]\} \quad (20)$$

where

$$f_s(|z-z_0|) = 2C_w + \gamma + i\pi/2 + \ell n[(k|z-z_0|) + \sqrt{(k|z-z_0|)^2 + \exp(-2\gamma - 2g)}] \quad (21)$$

C_w and γ are given in (11) and,

$$g = 33.88\ (ka)^2 \exp\left(-\frac{3.26}{ka}\right) \quad (22)$$

From (18) and (20), the input conductance of an infinitely long cylinder is then given by

$$G_\infty(ka) \approx \text{Re}\{U_s(0)\} = \text{Re}\{[\frac{i}{\eta} \ell n(2C_w - g - i\pi/2) - \ell n(2C_w - g + i3\pi/2)]\} \quad (23)$$

It will be shown later in Section 4 that (23) yields a very good input conductance for an infinitely long cylinder as thick as $ka = 1.0$. Also, we note that $U_s(z)$ in (20) is asymptotic to both forms of $U(\pi;z)$ in (9) and (13) for large kz and differs only in the vicinity of the source, $kz \approx 0$.

3.3 Secondary current on a semi-infinite receiving antenna

The secondary current on the external wall of a semi-infinite receiving cylinder (see Figure 3a), arises from the reflection of the current

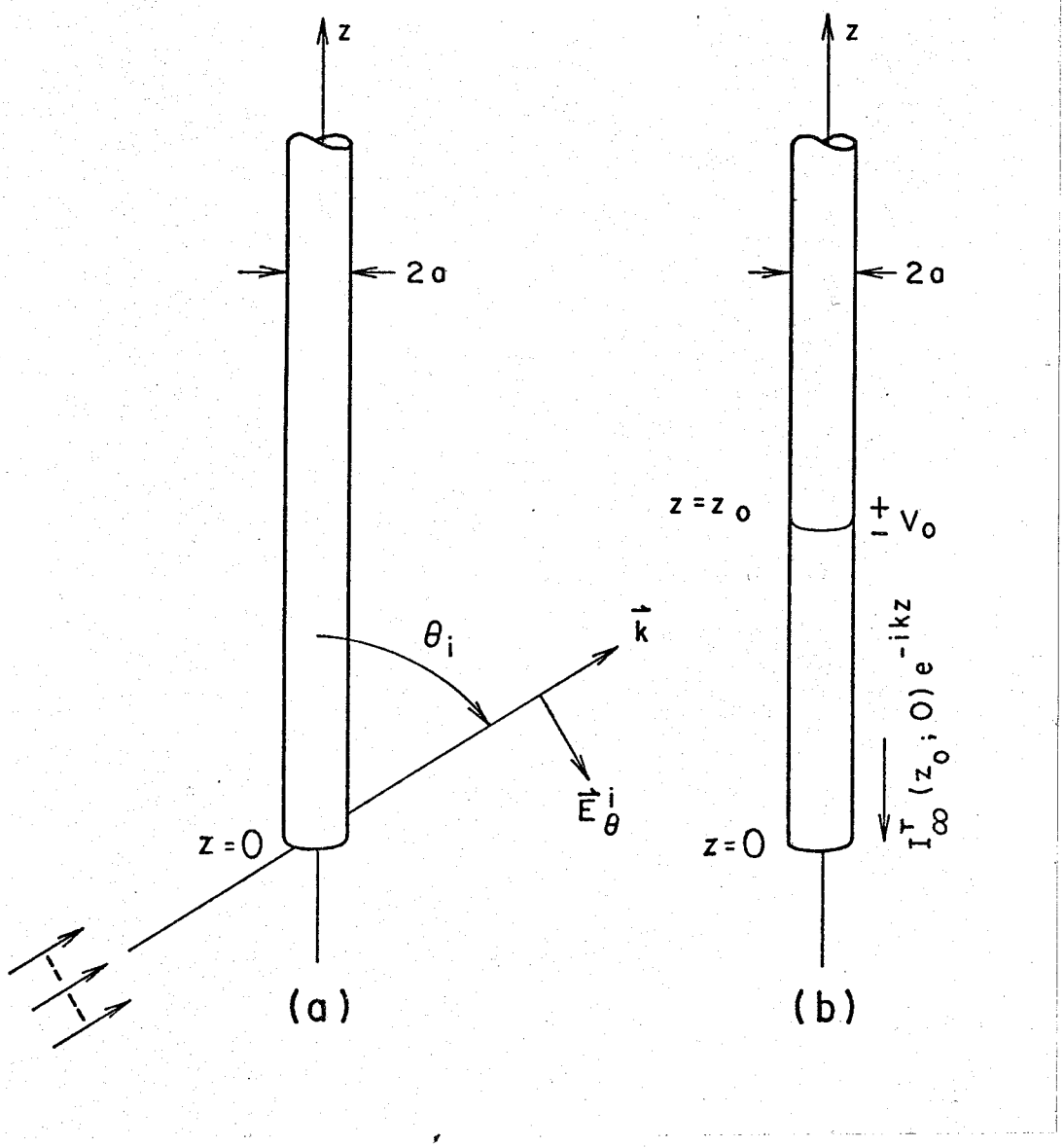

Figure 3. Semi-infinite tubular cylindrical antennas

a. receiving; uniform plane wave incident at an angle, θ_i, with respect to the z (antenna) axis.

b. transmitting, delta function voltage source of strength, V_0 volts, located at $z = z_0$.

$I_{\infty}^{R}(\theta_i,z)$ in (15) from the end of the cylinder. From a Wiener-Hopf analysis this reflected current may be expressed as [17, Eq. 27],

$$I_{refl}^{R}(\theta_i,z) = E_{\theta}^{i}\, V(\theta_i;0)\ \frac{ik}{2\pi}(1-\cos\theta_i)K_{+}(-k\cos\theta_i)$$

$$\int_{\Gamma_0} \frac{K_{+}(-\alpha)\, e^{-i\alpha z}}{(k+\alpha)(k\cos\theta_i+\alpha)K(\alpha)}\, d\alpha\ ;\quad 0 \le z < \infty \qquad (24)$$

$$0 \le \theta_i \le \pi$$

The contour Γ_0 is shown in Figure 1, and as previously noted, $K_{+}(\alpha)$ comes from the factorization of $K(\alpha)$ in (4) into functions analytic in the upper and lower halves of the complex α plane, i.e., $K(\alpha) = K_{+}(\alpha)K_{-}(\alpha)$. This factorization is more fully discussed in Appendix C. The superscript R in (24) signifies the receiving situation. We may write (24) in terms of the auxiliary canonical integral $W(\theta_i;z)$ in (6), and by virtue of (7), we have the approximate expression,

$$I_{refl}^{R}(\theta_i,z) \approx -E_{\theta}^{i}\, V(\theta_i;0)R(\theta_i)U(\theta_i;z);\quad 0 < z < \infty\ ,$$

$$0 \le \theta_i \le \pi \qquad (25)$$

where we have defined the "reflection coefficient",

$$R(\theta_i) = \frac{\eta}{2\pi} K_{+}(k)K_{+}(-k\cos\theta_i) \qquad (26)$$

The approximate expression for the reflected current in (25) is valid if the basic condition in (8) is satisfied. We note that the reflected current distribution considered here is, as in the primary receiving current distribution in Section 3.1, the total z-directed current averaged over the circumference of the cylinder.

One of the obstacles, which in the past has prevented the practical

application of the Wiener-Hopf technique to thicker antennas, has been the absence of a tractable expression for $K_+(\alpha)$ in the range $-k \le \alpha \le k$ which appears in (26). It is shown in Appendix C, that a curve fitting procedure involving the factor, $K_+(\alpha)$, with compensation for its dominant irregularity, yields the approximate formula,

$$K_+(\alpha) = \begin{cases} \dfrac{K_+^0(\alpha)}{|A|[1 + B_r(\frac{\alpha}{k})]} & ; \ 0 \le \alpha \le k \\ \dfrac{K_+^0(\alpha)}{|A|[1 + B_r(\frac{\alpha}{k}) + C(\frac{\alpha}{k})^2]} & ; \ -k \le \alpha \le 0 \end{cases} \tag{27}$$

where $K_+^0(\alpha)$ is the small argument form of $K_+(\alpha)$ based upon the assumptions that $ka << 1$ and $\alpha a << 1$ [1, Sec. 38] given by

$$K_+^0(\alpha) = \sqrt{2C_w + i\pi}\ [1 - \frac{1}{2C_w + i\pi} \ln(\frac{k+\alpha}{2k})] \ . \tag{28}$$

$|A|$ is the magnitude of A given by,

$$A = K_+^0(0)[i\pi J_0(ka)H_0^{(1)}(ka)]^{-1/2} \ . \tag{29}$$

B_r is given by

$$B_r = \frac{\eta}{2\pi} G_\infty(ka) - \mathrm{Re}\{[2C_w + i\pi + \ln(2)]^{-1}\} \tag{30}$$

and is the real part of a more complicated function, B, given in (C19) in Appendix C. Here $G_\infty(ka)$ is the input conductance of an infinite cylindrical antenna having an electrical radius, ka, for which we have the approximate formula given in (23). Appendix B gives a detailed discussion

of the exact and approximate forms of $G_\infty(ka)$. And finally, the coefficient C is given in terms of $|A|$ and B_r by,

$$C = \frac{1 - |A|^2(1 - B_r^2)}{|A|^2 (1 + B_r)} \tag{31}$$

Although (27) is basically a curve-fit solution for $K_+(\alpha)$ in the range, $-k < \alpha \leq k$, the coefficients $|A|$ and B_r were obtained in much the same manner as those in a two-term Taylor series expanion of $K_+^0(\alpha)/K_+(\alpha)$ in the upper-half of the complex α-plane. The coefficient, C, was obtained by requiring that the approximate constructed quantity $K(\alpha) = K_+(\alpha)K_-(\alpha)$ (see (C5) and (C6) of Appendix C) using (27) have the same limiting form as the exact $K(\alpha)$ in (4) as $\alpha \to \pm k$.

3.4 Secondary current on a semi-infinite transmitting antenna

The secondary current eminating from the end at $z = 0$ of a semi-infinite, $0 \leq z < \infty$, cylinder having a delta function voltage source of strength V_0 at $z = z_0$ is usually approximated by the reflection of a wave incident at $\theta_i = \pi$ [6], as illustrated in Figure 3b. Hence, from (24) we may write,

$$I^T_{refl}(z_0;z) = -I^T_\infty(z_0;0)R(\pi)U(\pi;z) \qquad , 0 < z < \infty \tag{32}$$

where we have replaced the receiving incident current, $E^i_\theta V(\theta_i;0)$ by the transmitting incident current, $I^T_\infty(z_0;0)$.

4. Numerical comparisons: infinite and semi-infinite antennas

4.1 Primary transmitting current

As discussed in Section 3.1, we shall use the modified Shen, et al. [6] formula denoted as $U_s(z)$ in (20) for the primary current on a cylindrical transmitting antenna. And since Shen has already compared his approximate expression with numerically "exact" data in [6] for values of ka up to 0.08 with good agreements, we shall only consider cases in which $0.1 \leq ka \leq 1.0$ to justify the extension of the theory to this range. In Figure 4, we show the real and imaginary components of the current distribution on an infinitely long cylinder as predicted by the modified Shen formula in (20) with $V_0 = 1$ volt, for the particular values of the electrical radii, ka = 0.1, 0.5, and 1.0. "Exact" data for these cases obtained from the numerical integration of (18) is also shown in Figure 4 (as circles). And it may be observed that the real component of the current distribution predicted by (20) compares very favorably with the exact numerical data over the entire range of kz shown especially for the smaller values of ka. The imaginary component of the current distribution predicted by (20) compares favorably with the exact data only when the ratio, 2z/a, somewhat exceeds unity.

As mentioned earlier, the purpose of Shen's and our curve-fitting procedures leading to (20) for the primary transmitting current was to obtain a good value for the real part of the current at the source, i.e., the input conductance of an infinitely long cylindrical antenna. To demonstrate the level of success attained in this respect we offer Figure 5, which shows the input conductance of an infinitely long cylinder as obtained from the real part of $U_s(0)$ in (23) and the "exact" numerically evaluated input conductance from the exact integral expression stated in (B1) of Appendix

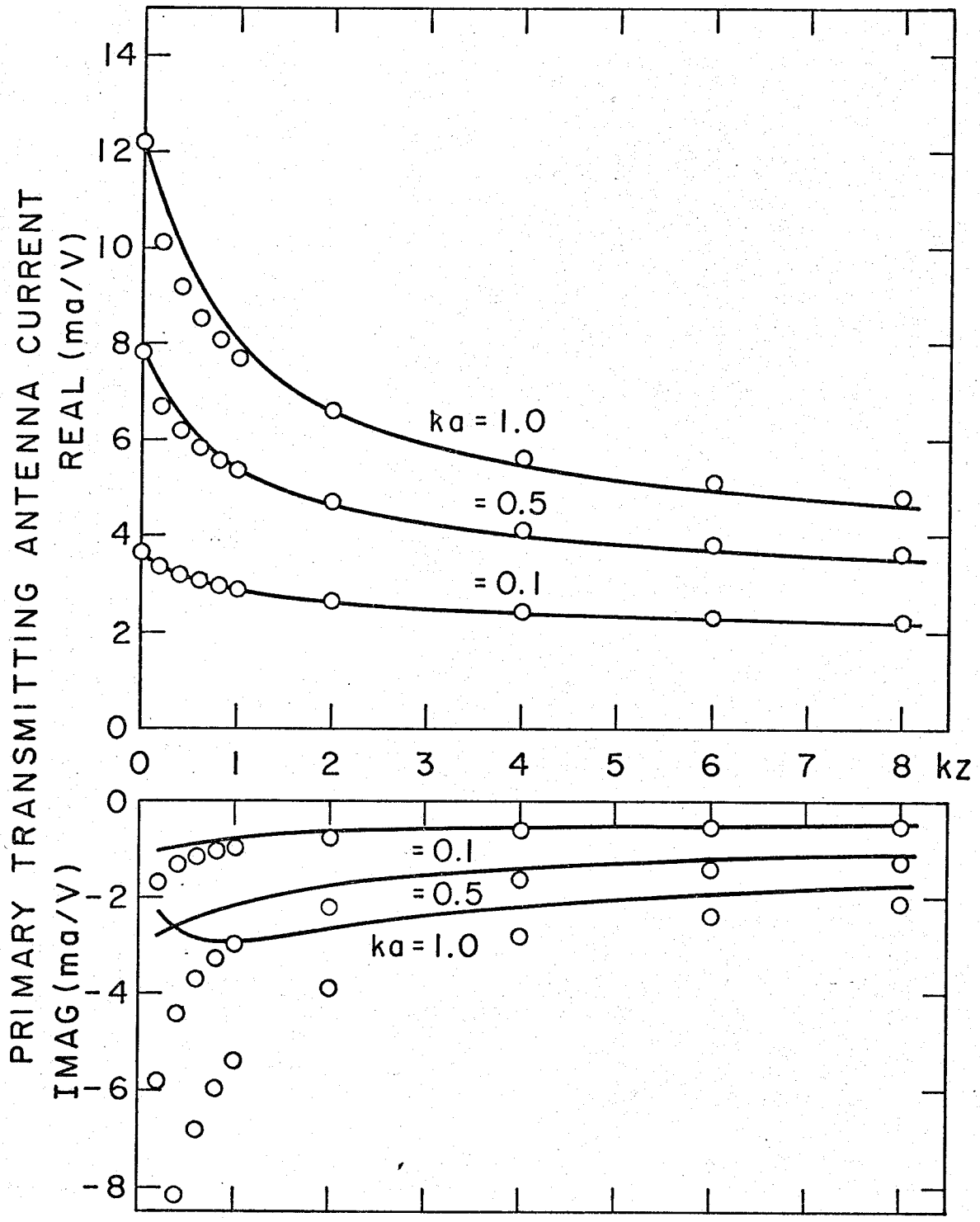

Figure 4. Current distribution on an infinitely long cylindrical transmitting antenna with a delta function voltage source at $z = z_0 = 0$.

———— Approximate distribution from the modified Shen [6] formula denoted by $U_s(|z - z_0|)$ in eq. (20).

o "Exact" numerically evaluated data from eq. (18).

Note: The traveling wave factor, e^{ikz}, has been suppressed.

B as functions of ka over the range $10^{-4} \leq ka \leq 1$. Obviously, excellent agreement is obtained. In fact, the error, which is also shown in Figure 5, never exceeds 2% over the entire range.

4.2 Reflection coefficient $R(\theta_i)$

The behavior of the "exact" numerically evaluated (using the formula of Mittra and Lee [15, Sec. 5-2.(3)]) $K_+(\alpha)$ is shown in Figure 6 as a function of α in the range $-k < \alpha < k$ for the specific cases ka = 0.01, 0.05, 0.1, 0.5, and 1.0. This variation in α when $\alpha = -k \cos \theta_i$ corresponds to the range $0 < \theta_i < \pi$. The behavior of our approximate form of $K_+(\alpha)$ in (27) is so close to the exact we have not included this data in Figure 6 but have elected to show, in Figure 7, the error between the approximate and "exact" values of $K_+(\alpha)$ for the same range and set of parameters as those in Figure 6. The magnitude and phase error illustrated in Figure 7 is seen to be quite small, typically below 1% and $\pm 5^\circ$, respectively. And it should be noted, that this magnitude error is many times smaller than the magnitude error of the normally accepted small argument approximation, $K_+^0(\alpha)$ in (28). For example, at ka = 0.01 $K_+^0(k)$ differs from the exact value of $K_+(k)$ by about 1.5%, while our approximate form of $K_+(k)$ from (27) possesses an error of less than 0.1%. And as the value of ka increases, the error in $K_+^0(k)$ increases quite rapidly, reaching over 200% at ka = 1.

Obviously, the quantity of more crucial importance is the so-called "reflection coefficient", $R(\theta_i)$ in (26). Figure 8 shows the magnitude and phase of $R(\theta_i)$ as calculated using the "exact" numerically determined values of $K_+(k)$ and $K_+(-k \cos \theta_i)$ (again from the formula of Mittra and Lee [15, Sec. 5-2.(3)]) as a function of ka over the range $10^{-4} \leq ka \leq 1$ for the incident angles $\theta_i = \pi/36, \pi/4, \pi/2, 3\pi/4$ and π.

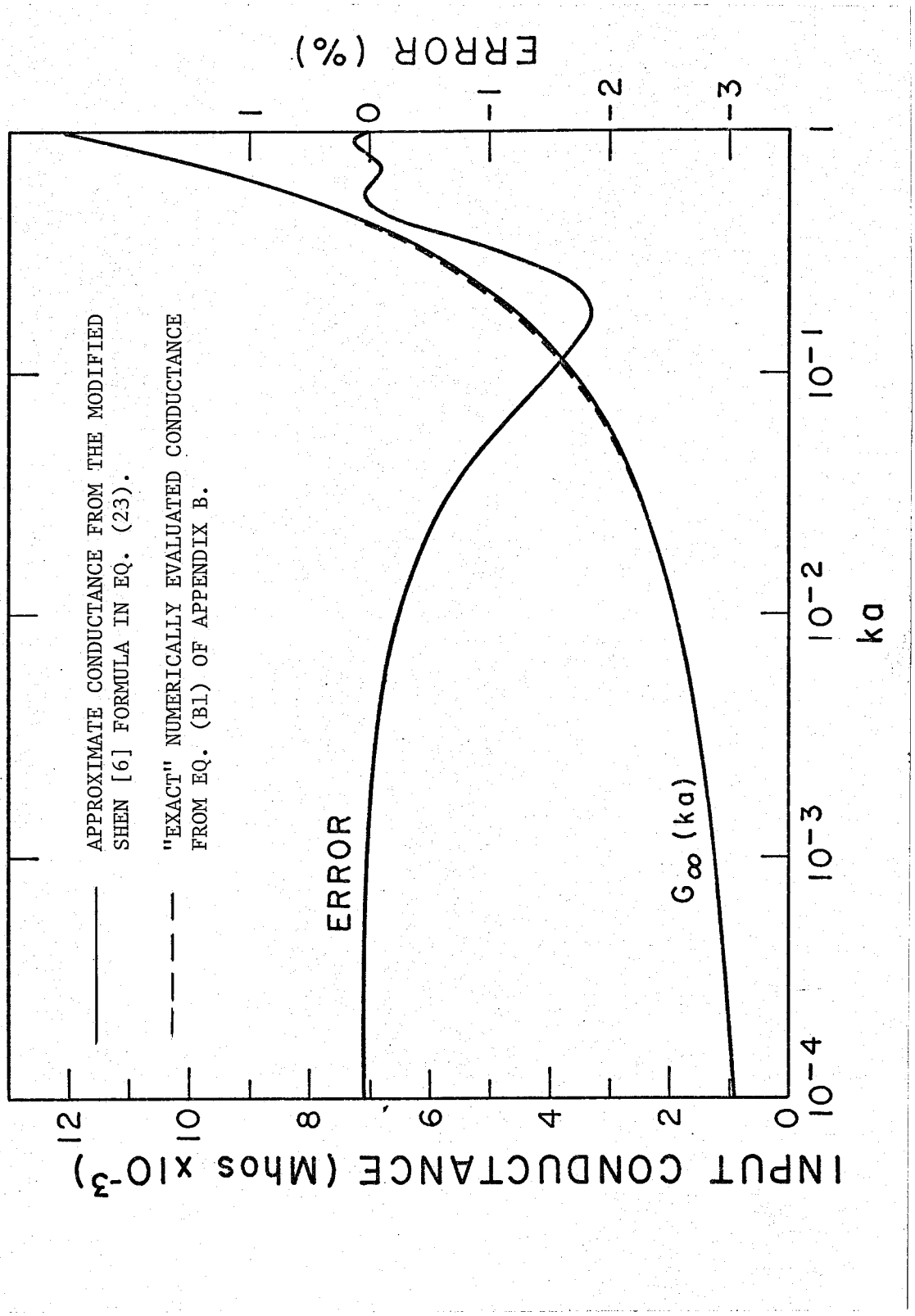

Figure 5. Input conductance of an infinitely long tubular cylinder.

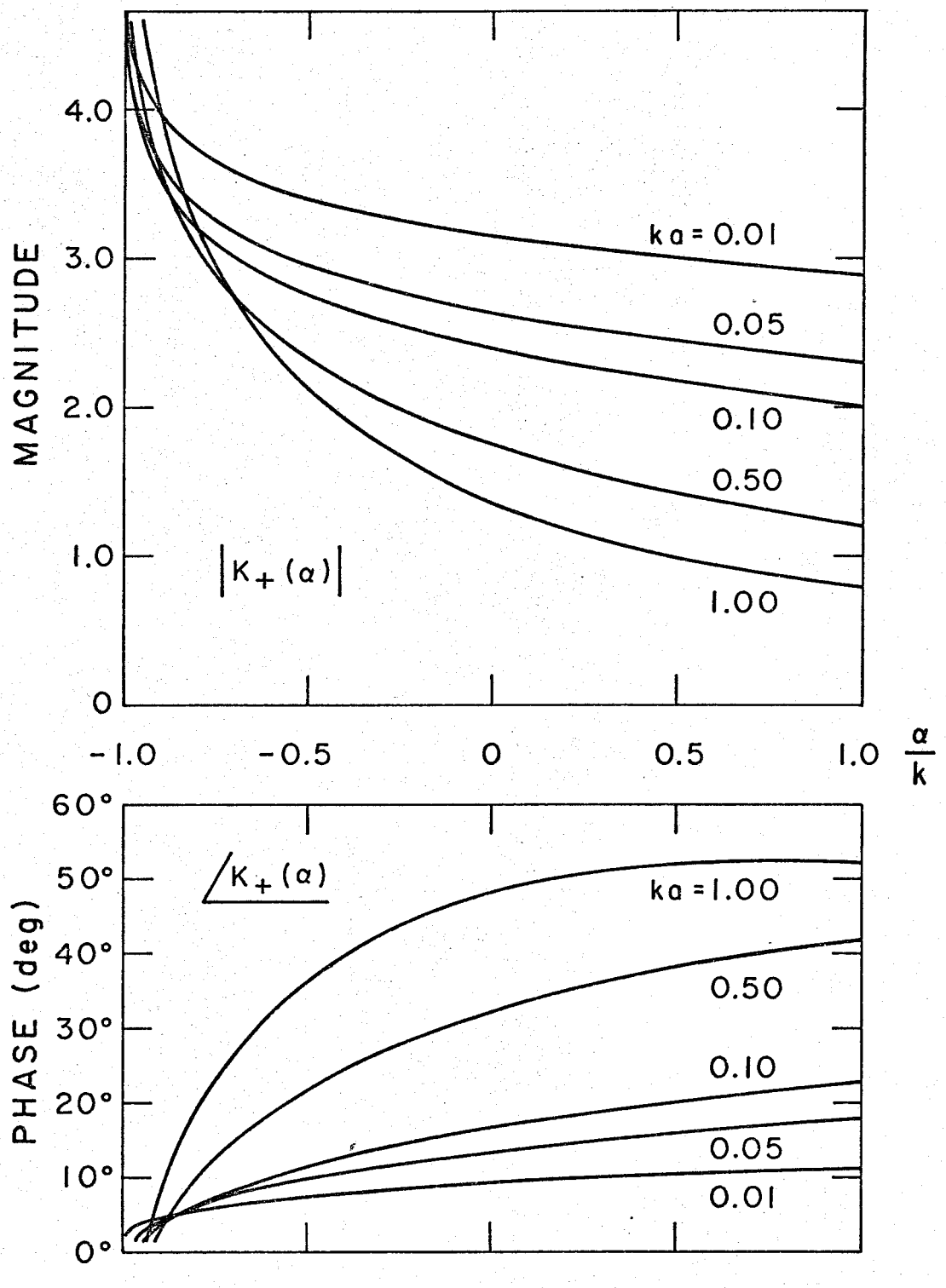

Figure 6. Magnitude and phase of $K_+(\alpha)$ in the range, $-k \leq \alpha \leq k$, calculated from the exact formula for $K_+(\alpha)$ in [15, 5-2,(3)], (See eq.(C11) of Appendix C of this report.)

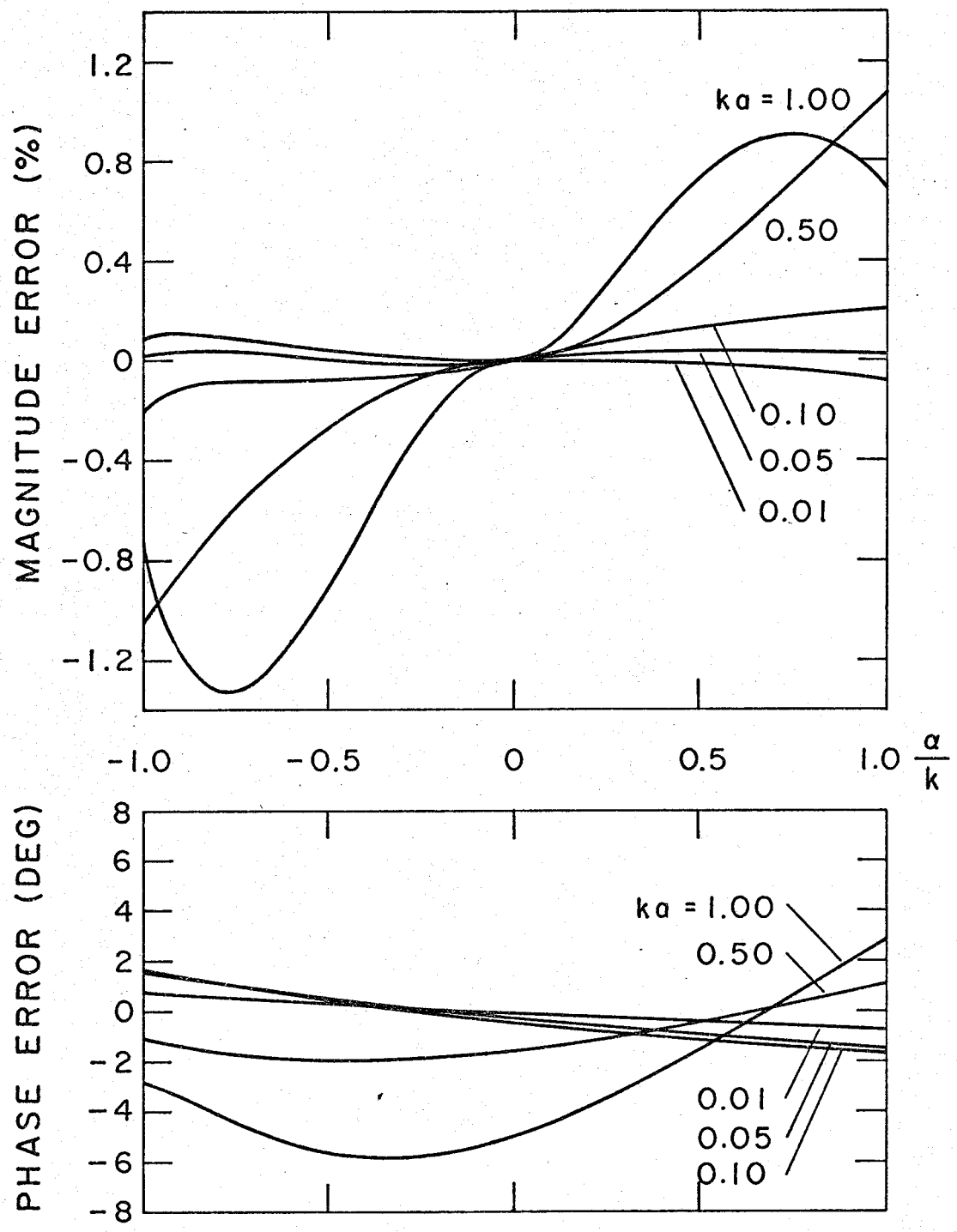

Figure 7. Magnitude and phase errors of the approximate form of $K_+(\alpha)$ in eq. (27) for the range $-k \leq \alpha \leq k$.

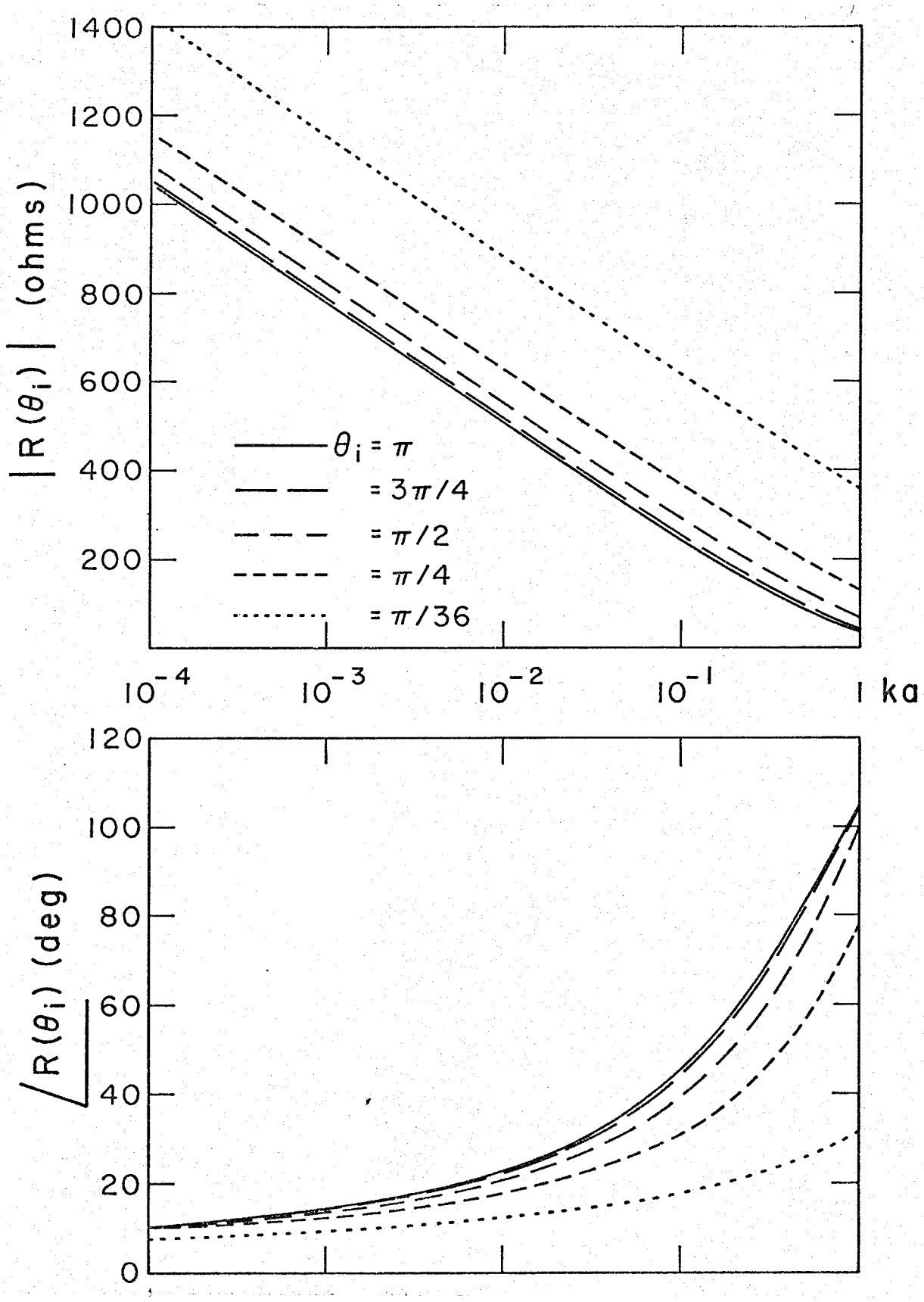

Figure 8. Magnitude and phase of the "reflection coefficient," $R(\theta_i) = (\eta/2\pi)K_+(k)K_+(-k\cos\theta_i)$, calculated from the exact formula for $K_+(\alpha)$ in [15, Sec 5-2.(3)] (See eq. (C11) of Appendix C of this report.)

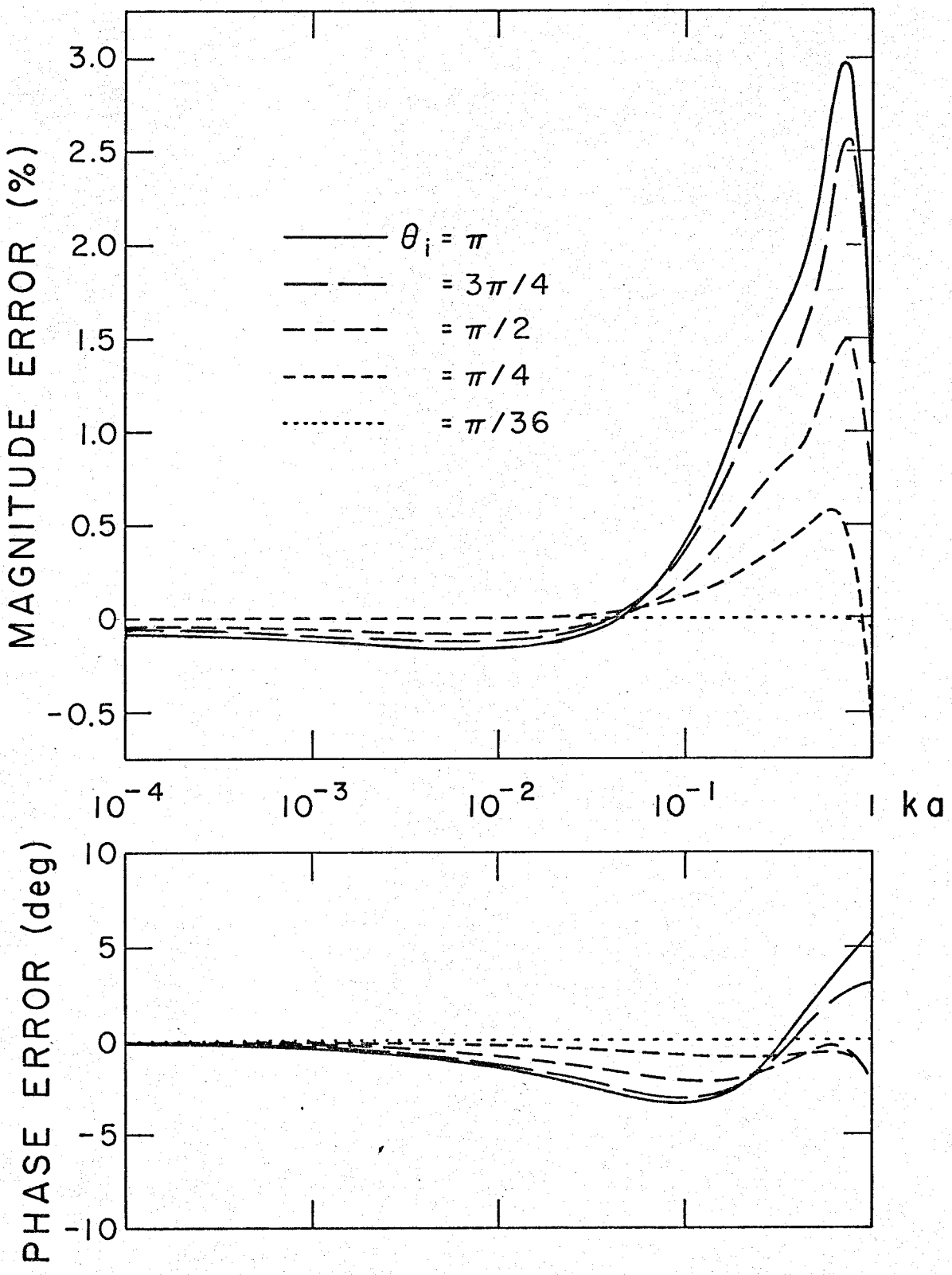

Figure 9. Magnitude and phase errors of the "reflection coefficient," $R(\theta_i) = (\eta/2\pi)K_+(k)K_+(-k \cos \theta_i)$, calculated using the approximate formula for $K_+(\alpha)$ in (27).

Data for $R(\theta_i)$ using the approximate formula for $K_+(\alpha)$ in (27) is not included in Figure 8 because of the very close agreement it has with the exact data. Instead, we show the error of this approximation with regard to the exact in Figure 9 for the same range and set of parameters as in Figure 8. The magnitude error is seen to be at most about 3% and typically much less while the very small phase error is never more than $\pm 5^\circ$.

4.3 Reflected current distributions

Denoting the reflected current due to a unit incident current of the form $\exp[ikz \cos \theta_i]$ as $I^N_{refl}(\theta_i;z)$, we have from (6) and (24) the expression,

$$I^N_{refl}(\theta_i,z) = -\frac{\eta}{2\pi} K_+(-k \cos \theta_i)\, W(\theta_i;z) \quad ; \; 0 \le z \le \infty, \; 0 \le \theta_i \le \pi \tag{33}$$

in both the receiving and transmitting situations. We note that (33) is an exact expression for the normalized reflected current in the receiving situation $(0 \le \theta_i \le \pi)$ and is a very good approximation for the normalized reflected current in the transmitting situation $(\theta_i = \pi)$ when the delta function voltage source is located sufficiently away from the end. From (7) and (26), the approximate form of (33) is given by

$$I^N_{refl}(\theta_i,z) = -R(\theta_i)U(\theta_i;z) \quad ; \; 0 \le z \le \infty, \; 0 \le \theta_i \le \pi \tag{34}$$

To demonstrate the accuracy attained with our approximate formulas, Figures 10-14 show the behaviors of the "exact" reflected currents in (33) (with $K_+(-k \cos \theta_i)$ numerically determined using the formula of Mittra and Lee [15, Sec. 5-2.13] and $W(\theta_i;z)$ in (6) numerically integrated) and

Legend for Figures 10-14

○ $\theta_i=\pi$
□ $=\pi/2$
⬡ $=\pi/4$
△ $=\pi/36$

"Exact" numerically determined $I^N_{refl}(\theta_i;z)$ from (33) found by using the formula of Mittra and Lee [15, Sec. 5-2.(3)] for $K_+(\alpha)$ and by the numerical integration of $W(\theta_i;z)$ given in (6).

———— Approximate form of $I^N_{refl}(\theta_i;z)$ given in (35), with $R(\theta_i)$ from (26) determined by the approximate $K_+(\alpha)$ formula in (27) and the approximate formula (13) used for $U(\theta_i;z)$.

— — — Approximate form of $I^N_{refl}(\theta_i;z)$ given in (35), with $R(\theta_i)$ from (26) determined by the approximate $K_+(\alpha)$ formula in (27) and the approximate formula in (9) used for $U(\theta_i;z)$.

Note: In Figures 10-14, the traveling wave phase factor, e^{ikz}, has been suppressed to aid in improving the clarity of the information presented.

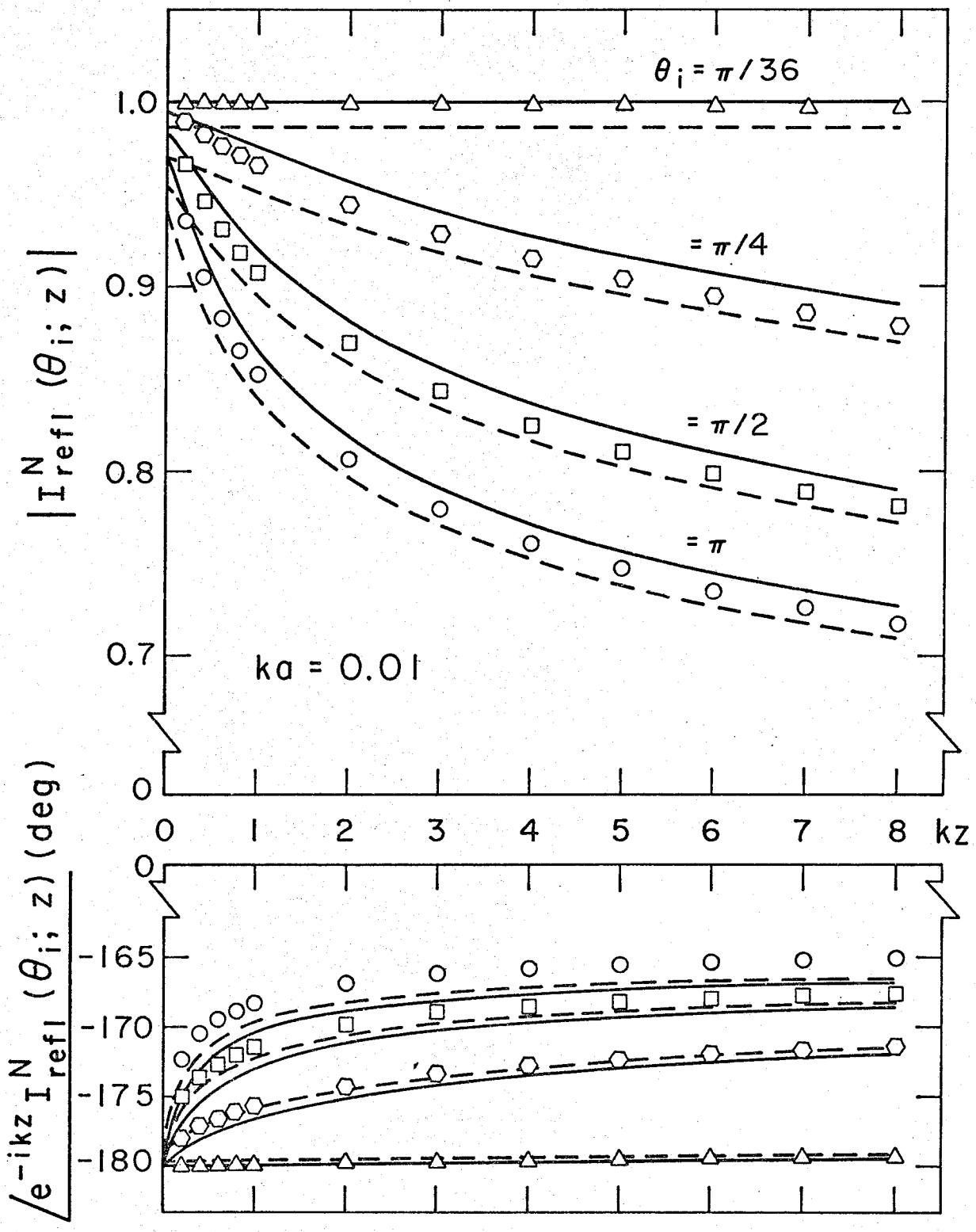

Figure 10. Magnitude and phase of the current reflected from the end of a semi-infinite tubular cylinder where ka = 0.01. (See accompanying Legend for further details.)

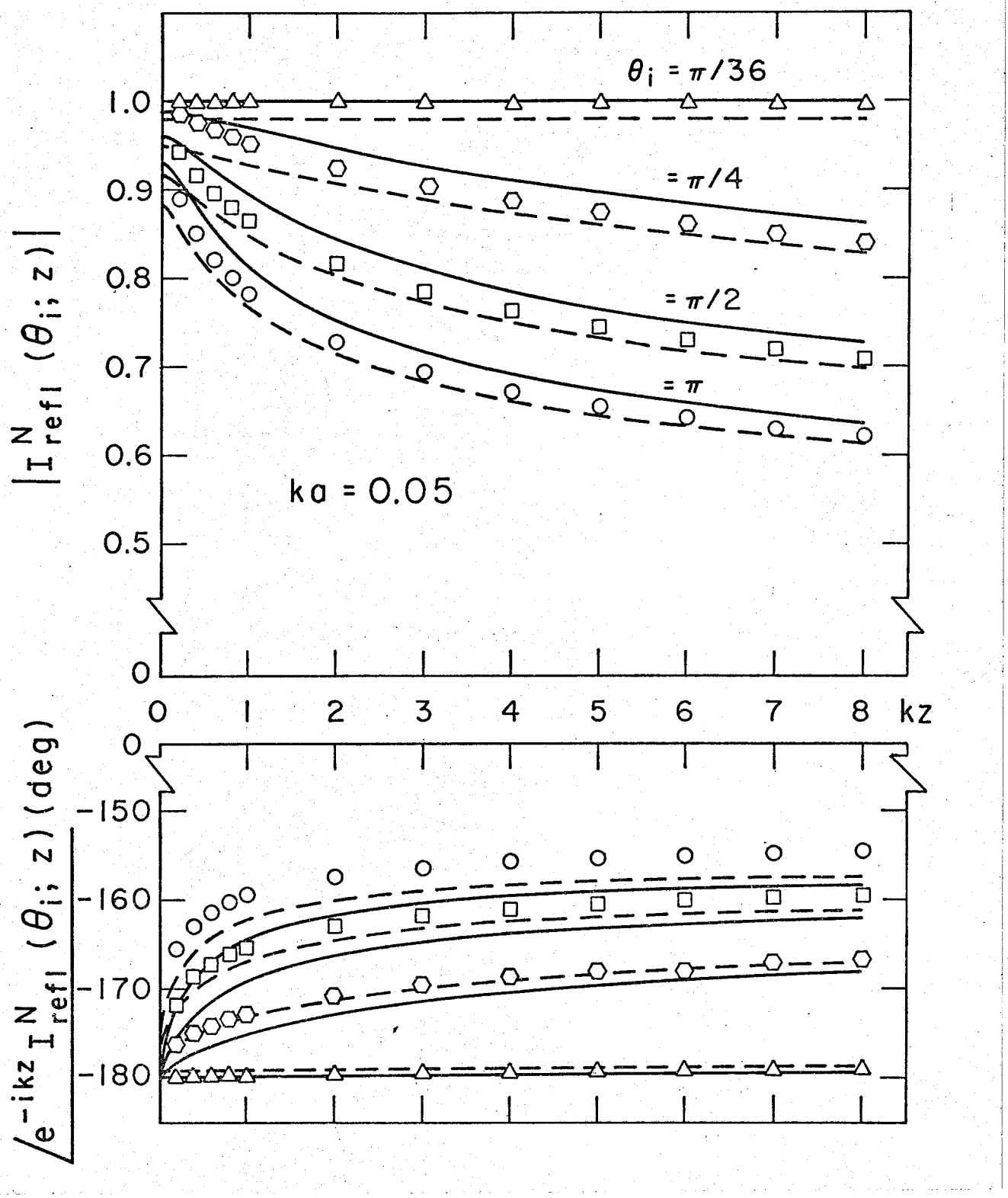

Figure 11. Magnitude and phase of the current reflected from the end of a semi-infinite tubular cylinder where ka = 0.05. (See accompanying Legend for further details.)

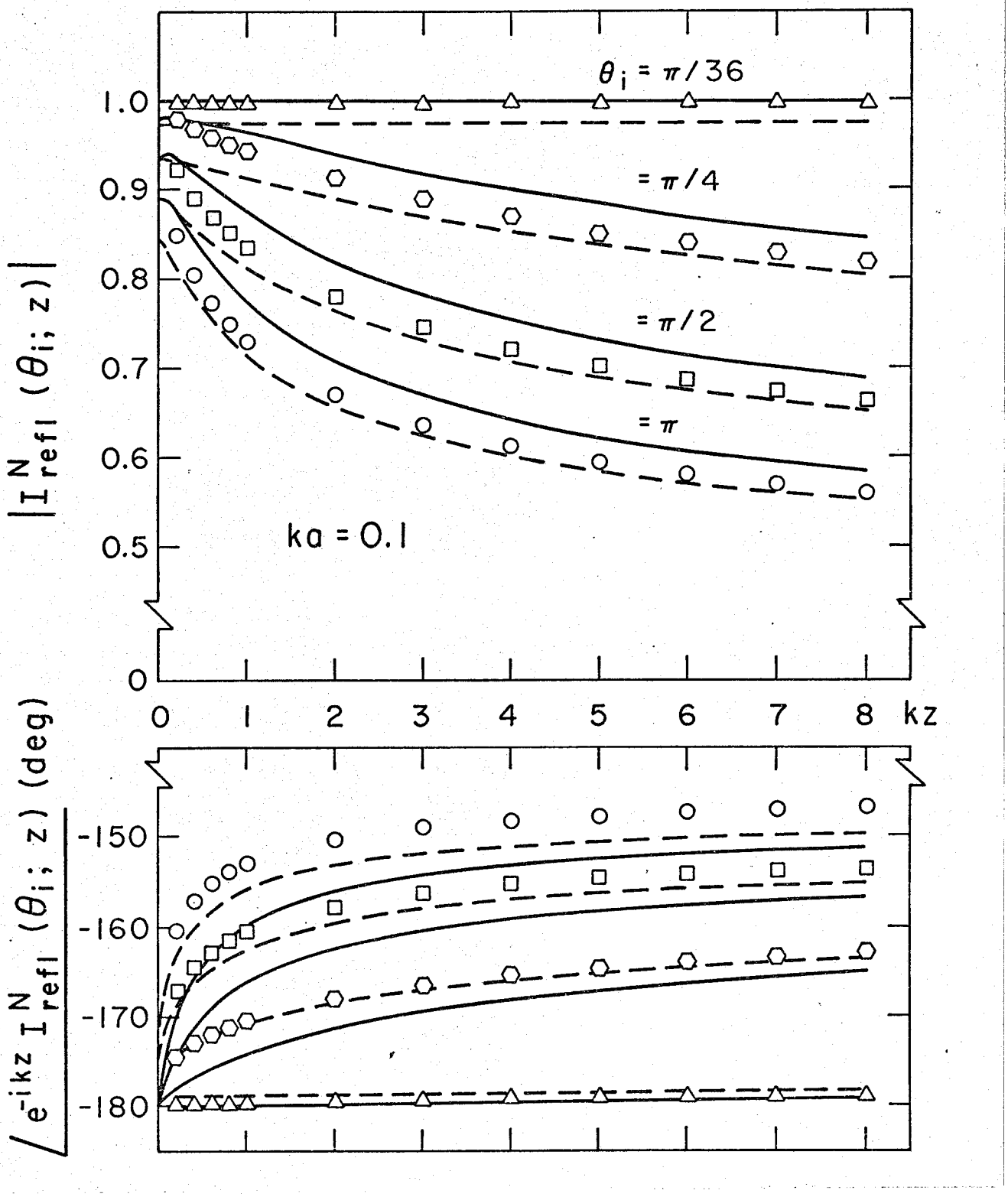

Figure 12. Magnitude and phase of the current reflected from the end of a semi-infinite tubular cylinder where ka = 0.1. (See accompanying Legend for further details.)

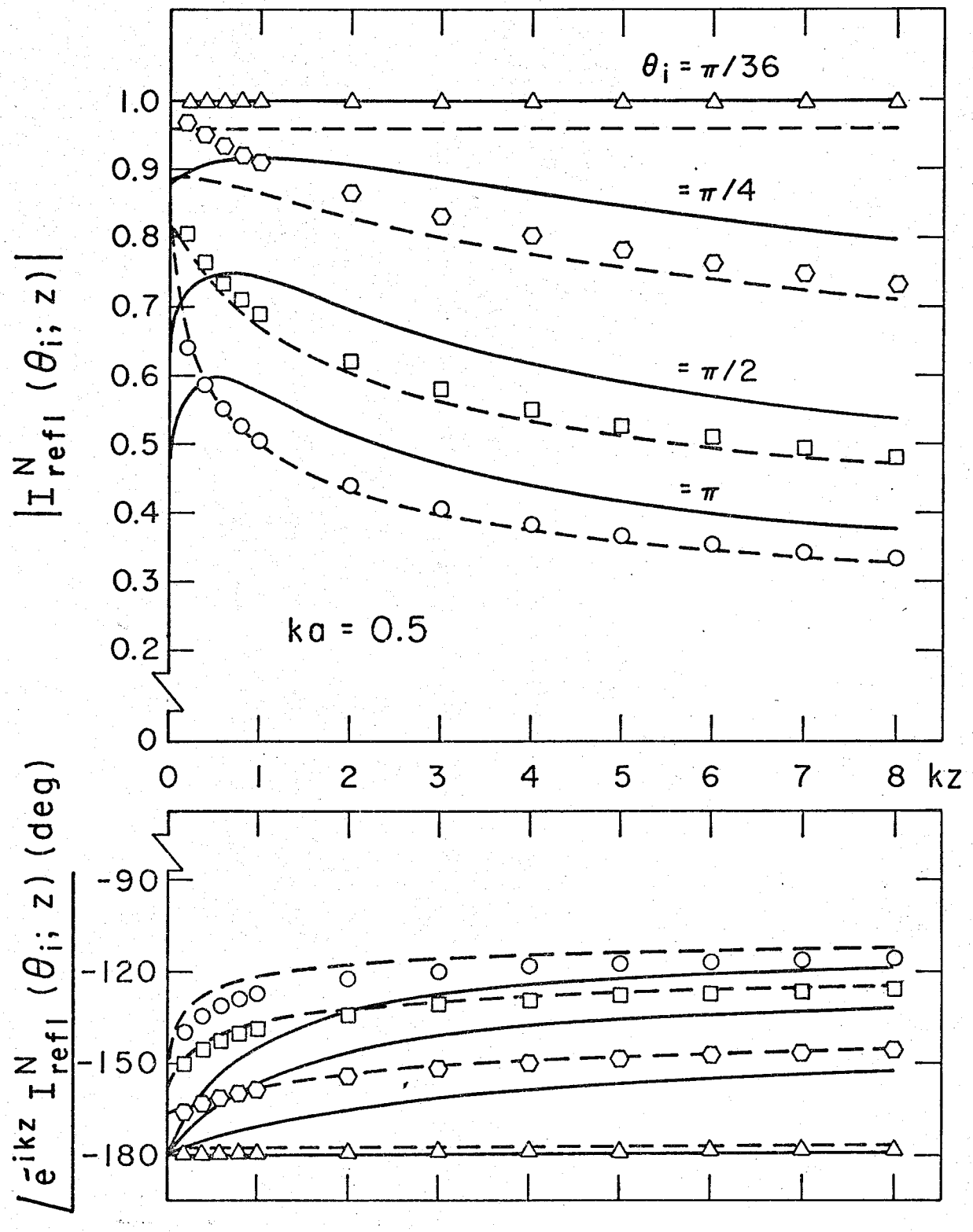

Figure 13. Magnitude and phase of the current reflected from the end of a semi-infinite tubular cylinder where ka = 0.5. (See accompanying Legend for further details.)

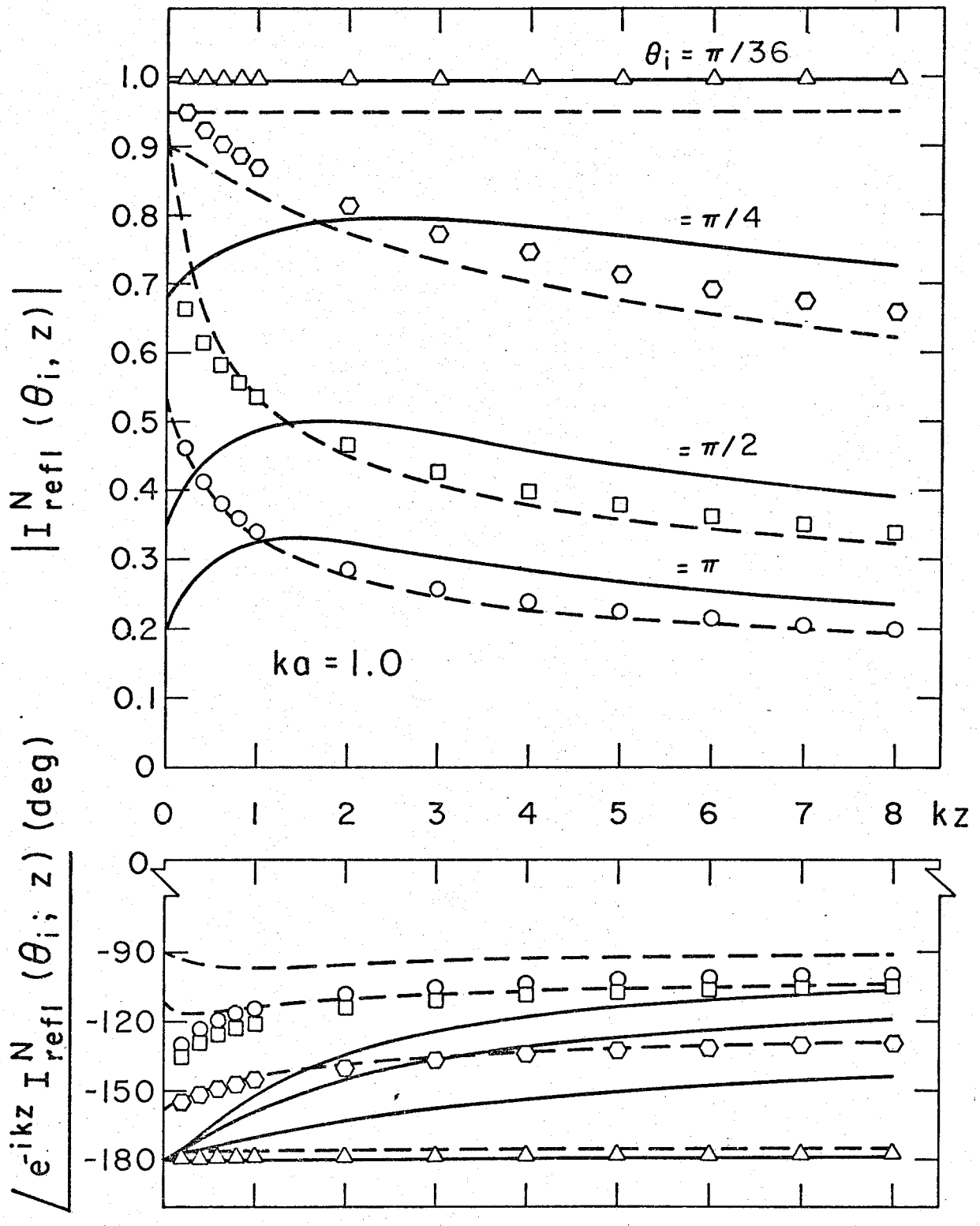

Figure 14. Magnitude and phase of the current reflected from the end of a semi-infinite tubular cylinder where ka = 1.0. (See accompanying Legend for further details.)

the approximate reflected currents in (34) using (27) for $K_+(\alpha)$ in (26) for $R(\theta_i)$ and using both (9) and (13) for $U(\theta_i;z)$ as function of kz in which $\theta_i = \pi/36, \pi/4, \pi/2,$ and π for the values of ka equal to 0.01, 0.05, 0.1, 0.5, and 1.0, respectively. We note that in every case, the data obtained from the use of (9) for $U(\theta_i;z)$ appears to be closer to the numerical data than does results using (13) for $U(\theta_i;z)$. This is somewhat misleading, since in the finite length cylinder situation where multiple reflections of currents from the end are characterized by waves incident at an angle, $\theta_i = \pi$, and subsequently summed (see Section 5) slightly better results are obtained with (13) used for $U(\theta_i;z)$. This apparent incongruity must be a result of the summation procedure producing an error which is more compensitive for the error in (13) for $U(\theta_i;z)$ than it is for the error in (9). A more detailed clarification of this point will be forthcoming.

Section 5. Approximate expressions for the external currents on finite-length cylindrical antennas

Expressions for the currents on finite length cylindrical antennas are constructed by summing the primary and subsequent secondary currents reflected from the ends of the antenna.

5.1 Finite receiving antenna

Our theory can now be applied to the finite length receiving antenna with the understanding that only the average (over the circumference) z-directed current is obtained. As noted by Kao [18] specifically for normal incidence of the plane wave, this zero-order current is not coupled to any higher order variations of the current with respect to the azimuthal angle, ϕ, and may be considered independently from these higher order currents. Rispin and Chang [19] have also noted this to be true for arbitrary polarization and arbitrary incidence of the uniform plane wave.

The constituative currents on a finite length ($-h \le z \le h$), cylindrical receiving antenna with radius, a, are shown pictorially in Figure 15. Beginning with the plane wave induced primary current, $E^i_\theta V(\theta_i;z)$, shown in Figure 15a, the reflections of this current from the end at $z = -h$ and the $z = +h$ end are determined to be $-V(\pi-\theta_i;h)R(\theta_i)U(\theta_i,h+z)$ and $-V(\theta_i;h)R(\pi-\theta_i)U(\pi-\theta_i,h-z)$, respectively, as illustrated in Figure 15b. These reflected currents then propagate toward opposite ends of the cylinder (analogous to waves incident at an angle π with respect to a particular end) at which point they reflect again as $-V(\pi-\theta_i;h)R(\theta_i)U(\theta_i;2h)$ $R(\pi)U(\theta;h-z)$ and $-V(\theta_i;h)R(\pi-\theta_i)U(\pi-\theta_i;2h)R(\pi)U(\pi;h+z)$, respectively. Continuing this procedure leads to an infinite number of reflected currents eminating from each end of the cylinder, as suggested in Figure 15c. The infinite series expressing the current reflected from a particular end of

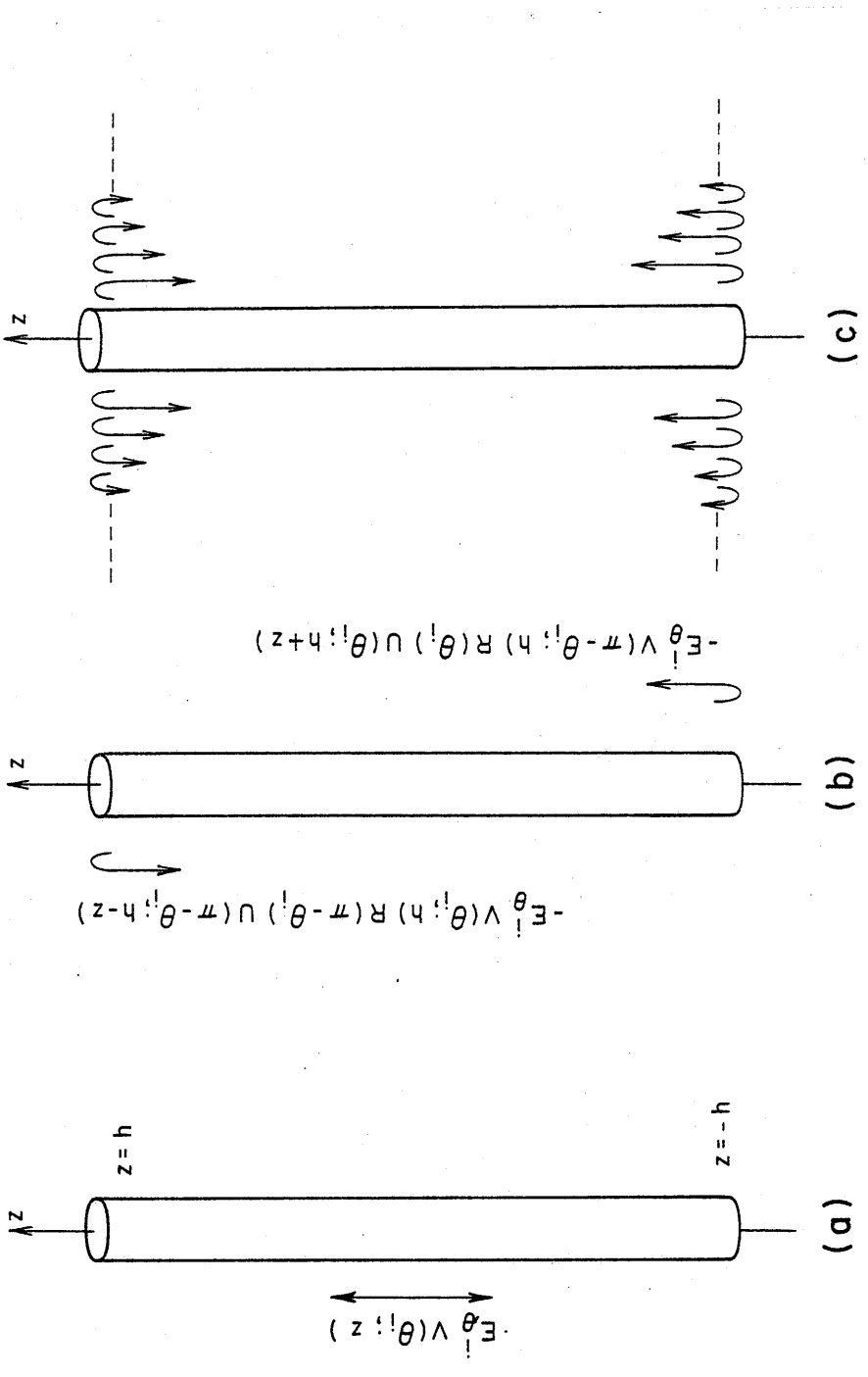

Figure 15. Illustration of the multiple reflection concept as applied to the finite length cylindrical receiving antenna.

a. Primary receiving current distribution from eq. (15).

b. Initial reflection of the primary current from each end from eq. (25).

c. Subsequent multiple reflections.

the cylinder are in the form of simple geometric series which may be readily summed. Hence, we arrive at the following expression for the total external current on the finite length cylindrical receiving antenna,

$$I^R(\theta_i;z) = E^i_\theta\{V(\theta_i;z) - V(\pi-\theta_i,h)R(\theta_i)U(\theta_i;h+z) - C^R(\pi-\theta_i)R(\pi)U(\pi,h+z)$$

$$- V(\theta_i;h)R(\pi-\theta_i)U(\pi-\theta_i,h-z) - C^R(\theta_i)R(\pi)U(\pi,h-z)\} \qquad (35)$$

where

$$C^R(\theta_i) = \frac{[V(\theta_i;h)R(\pi-\theta_i)U(\pi-\theta_i;2h)R(\pi)U(\pi;2h)-V(\pi-\theta_i;h)R(\theta_i)U(\theta_i;2h)]}{1 - [R(\pi)U(\pi;2h)]^2} \qquad (36)$$

represents the total incident current (with an analogous wave incidence of $\theta_i = \pi$) upon the end $z = +h$ due to current reflections eminating from the end at $z = -h$. $C^R(\pi-\theta_i)$ has a similar interpretation with the ends interchanged. The terms involving $R(\theta_i)U(\theta_i,h+z)$ and $R(\pi-\theta_i)U(\pi-\theta_i;h-z)$ represent the initial reflections of the primary current wave incident at the angles, θ_i and $\pi - \theta_i$, respectively. Thus, except for the primary term, $V(\theta_i;z)$, all the other terms in (35) represent reflected currents from the ends of the cylinder. Our expression for the receiving antenna current in (35) agrees in form with that of Weinstein [2] and can be shown to be consistent with our earlier result in [17] under the conventional thin wire approximations. A complete formal agreement between our result and that of Shen [7] occurs only when the terms $U(\theta_i;z)$ and $U(\pi-\theta_i,z)$ in (35) are approximated by $U_s(z)$ in (20) with the constant, g, deleted. The approximation of these terms in this manner is implicit in Shen's [7] analysis.

The limiting form of the current on a finite length receiving antenna as the angle, θ_i, approaches grazing incidence, i.e., $\theta_i \to 0$ or π, based upon both approximate forms of $U(\theta_i;z)$ in (9) and (13) is discussed in Appendix D. And it is found that, while our theory is not expected to be valid in this range because of the apparent violation of the restriction, $\Omega(z) >> |\ln(v_0)|$ in (8), the approximate form of $U(\theta_i;z)$ in (13) actually produces the very physically acceptable result of a vanishing current as $\theta_i \to 0$ or π. Also a smaller, magnitude-wise, result for the current near the ends of a cylinder for a fixed incident angle, θ_i, is obtained in Appendix D, when (13) is used for $U(\theta_i;z)$ rather than (9). These considerations are very important in the cases when the incident angle θ_i is near grazing, i.e., $\theta_i = 0$ or π, and when the length of the antenna becomes electrically short.

And, finally, we note the symmetrical behavior of (35) with respect to the incident angle of the uniform plane wave and the position, z,

$$I^R(\theta_i;-z) = I^R(\pi-\theta_i;+z) \tag{37}$$

5.2 Finite transmitting antenna

In much the same manner, the current on a finite length $(-h \le z \le +h)$ cylindrical transmitting antenna of radius, a, due to a delta function voltage source of strength, V_0, at $z = z_0$ (see Figure 16) may be expressed in terms of a primary current and the multiply reflected currents from the ends. Figure 16a illustrates the primary current, which we shall approximate by $U_s(|z-z_0|)$ from (20), eminating from the delta function voltage source at $z = z_0$. These waves are incident upon the ends of the cylinder at an angle of π respective to the particular end. Hence, the initial reflections of the primary current from $z = -h$ and $z = +h$ are,

$-V_0 U_s(\pi, h+z_0)R(\pi)U(\pi,h+z)$ and $-V_0 U_s(\pi, h-z_0)R(\pi)U(\pi,h-z)$, respectively, as is shown in Figure 16b. The reflections of these currents from the respective opposite ends and the subsequent reflections which follow (Figure 16c) lead to a pair of infinite series, which are again summable. The final result for the transmitting current distribution is given by,

$$I^T(z_0;z) = V_0\{U_s(|z-z_0|)$$

$$- U_s(h+z_0)R(\pi)U(\pi;h+z) - C^T(h+z_0)R(\pi)U(\pi;h+z)$$

$$- U_s(h-z_0)R(\pi)U(\pi;h-z) - C^T(h-z_0)R(\pi)U(\pi;h-z)\} \qquad (38)$$

where

$$C^T(z) = \frac{U_s(z)[R(\pi)U(\pi;2h)]^2 - U_s(2h-z)R(\pi)U(\pi;2h)}{1 - [R(\pi)U(\pi;2h)]^2} \qquad (39)$$

represents the sum of the currents incident upon the $z = -h$ and $+h$ ends of the antenna when z is taken as $h+z_o$ and $h-z_o$, respectively, due to current reflections eminating from the opposite end. Note that the initial reflection of the primary current from each end is explicitly stated in (38), the overall form of the transmitting current expression being the same as that for the receiving current in (35). Our transmitting current expression in (38) can be shown to be equivalent in form to those of many other authors [1, Sec. 35.7], [2], [6] and others.

However, unlike the expressions of these authors, our expression is more general and flexible, since we claim it may be used for electrically short as well as electrically thick antennas as long as the basic condition in (8), $\Omega(z') = 2\ln(2z'/a) << |\ln(2kz')|$ is satisfied (note here

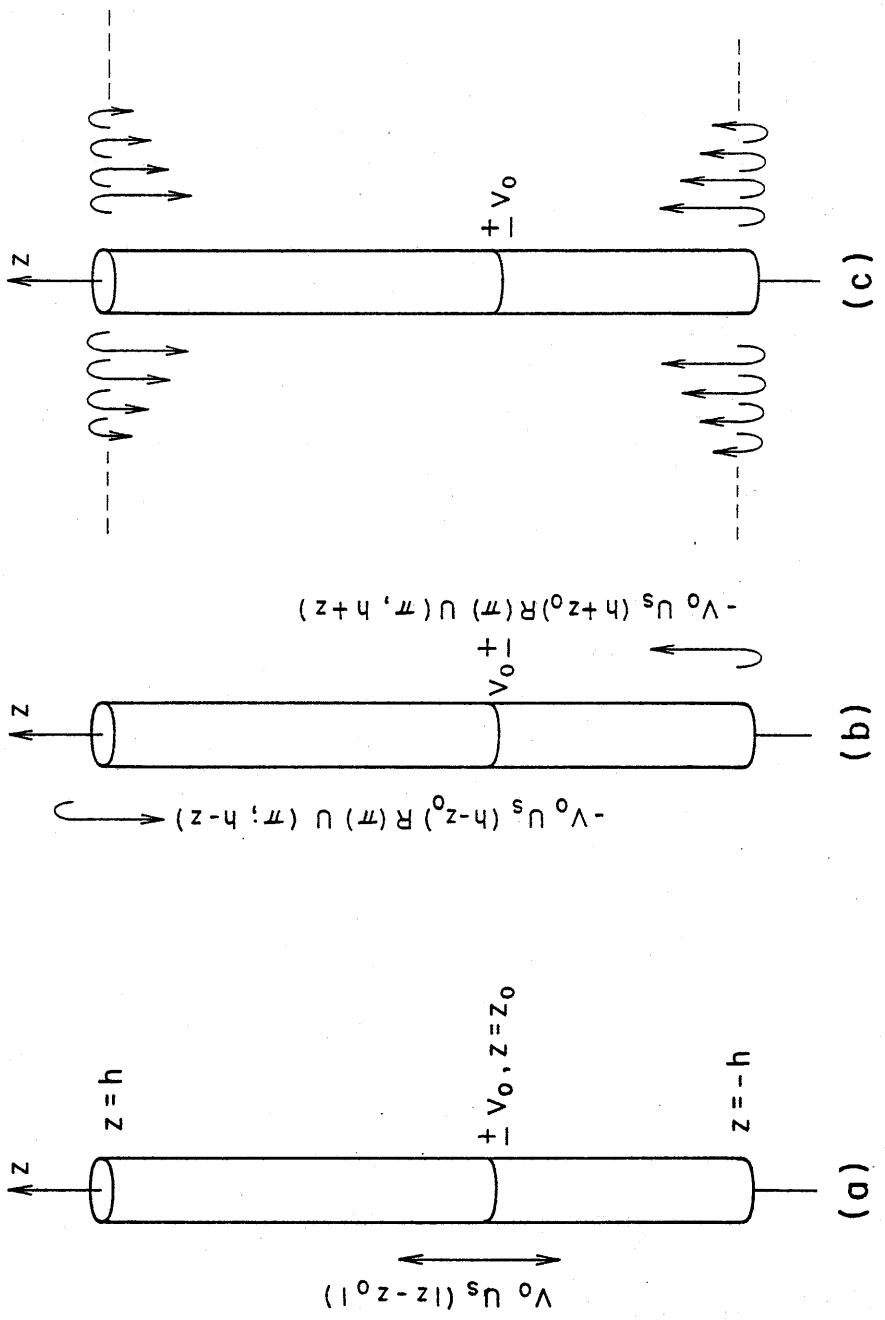

Figure 16. Illustration of the multiple reflection concept as applied to the finite length cylindrical transmitting antenna.

a. Primary transmitting current distribution from (19) and (20).

b. Initial reflection of the primary current from each end from eq. (32).

c. Subsequent multiple reflections.

z' refers to the distance to the source, $z-z_0$, and the distances to the cylinder ends, $h+z$ and $h-z$) and appropriately accurate values of $R(\pi)$ are used. And in this report, we often take the nominal measure, $z' = h$.

We note the symmetry in (38) with respect to the source and observation points, i.e.,

$$I^T(z_0;-z) = I^T(-z_0;z) \tag{40}$$

An approximate formula for the input admittance of an asymetrically driven cylindrical antenna of length, 2h, obtained by setting $z=z_0$ and $V_0 = 1$ volt in (38) is given by

$$\begin{aligned} Y_{in} = G - iB = U_s(0) \\ - U_s(h+z_0)R(\pi)U(\pi;h+z_0) - C^T(h+z_0)R(\pi)U(\pi;h+z_0) \\ - U_s(h-z_0)R(\pi)U(\pi;h-z_0) - C^T(h-z_0)R(\pi)U(\pi;h-z_0) \end{aligned} \tag{41}$$

Here G is the input conductance and B is a "relative" input susceptance. The qualification to a "relative" input susceptance is necessary, due to the fact we employ a delta function voltage source for the excitation and the mathematically predicted behavior of the imaginary part of the input current for this excitation should exhibit a logarithmic singularity [20] and [21]. This singularity would indicate an infinite capacitance, the so-called "knife-edge capacitance" [22]. However, the particular way in which the primary current term, $U_s(z)$, was derived (discussed in Section 3.2) does not allow the possibility of such a singularity in this current at the source. In a realistic sense, though, this slice

capacitance is due to an idealization in the mathematical model rather than a physically occurring phenomenon in the practical situation and in general does not pose any difficulties in experimental studies. Thus, the absence of such a singularity in our formulation is not unwelcomed.

6. Approximate expressions for the internal currents on cylindrical antennas

Thus far our theory has considered only the external current distributions on cylindrical antennas, hence, it is appropriate at this time to include a complementary discussion of the current distributions on the internal walls of receiving and transmitting cylindrical antennas. By combining the external and internal current distributions, the total current on the antenna may be found. But a more important use of a knowledge of the internal current occurs in some electromagnetic compatibility studies where it is desirable to know the amount of penetration into a long thin metallic enclosure. In many cases, the penetration is into the end of a cylinder and one needs to know the induced current on the internal wall of the cylinder.

6.1 Internal current on a semi-infinite receiving antenna

The TM_{0n} mode currents on the internal wall of a semi-infinite ($0 \le z \le \infty$) cylinder due to a plane wave incident at an angle, θ_i, are easily determined by a Wiener-Hopf analysis [17, Eq. 27] to be given by

$$\{I^R_{s\infty}(\theta_i;z)\}_{int} = E^i_\theta V(\theta_i;0)\ [\frac{ik}{2\pi}(1-\cos\theta_i)K_+(-k\cos\theta_i)]$$

$$\int_{\Gamma_1} \frac{K_+(-\alpha)e^{-i\alpha z}}{(k+\alpha)(k\cos\theta_i+\alpha)K(\alpha)}\,d\alpha\ ;\ 0 \le z \le \infty$$

$$0 \le \theta_i \le \pi \qquad (42)$$

where $E^i_\theta V(\theta_i;0)$ is the incident current at the end and is given in (15). The contour, Γ_1, is shown in Figure 1 and K_+ is the "plus" factor of $K(\alpha)$ in (4), which is discussed in Appendix C. Since the contour, Γ_1, encloses only simple poles of $[K(\alpha)]^{-1}$, the integral may be easily

evaluated and (42) may be written in the form,

$$\{I^R_{s\infty}(\theta_i;z)\}_{int} = E^i_\theta \, V(\theta_i;0) \sum_{n=1}^{\infty} T_{0n}(\theta_i) e^{-\gamma_{0n} z} \tag{43}$$

where T_{0n} is a transmission coefficient given by,

$$T_{0n}(\theta_i) = +i \frac{k}{2} (1-\cos\theta_i) K_+(-k\cos\theta_i) \frac{(\gamma_{0n}-ik)}{\gamma_{0n}(\gamma_{0n}+ik\cos\theta_i)} K_+(i\gamma_{0n}) \tag{44}$$

and,

$$i\gamma_{0n} = i\sqrt{(\rho_{0n}/a)^2 - k^2} \tag{45}$$

is the propagation constant of the TM_{0n} circular waveguide mode. And finally, ρ_{0n} is the n^{th} ordered zero of the Bessel function, J_0. Several approximations are possible to allow us to state the internal current in a more convenient form. The first of which is from the approximate splitting of the asymptotic form of the kernel, $K(\alpha)$, for large αa and is given by

$$K_+(\alpha) \approx \sqrt{i/(k+\alpha)a} \quad ; \quad \text{for } \alpha a \text{ large} \tag{46}$$

Numerical data comparing (46) with the exact value of $K_+(\alpha)$ from the formula of Mittra and Lee [15, Sec. 5-2.(3)] has shown good agreement for $\alpha \geq i\gamma_{01}$ up to $ka \approx 1.0$. Also for $e^{-\gamma_{0n} z} \ll 1$, the infinite sum may be truncated at $n=N$ and the subsequent loss of information for the smaller values of z may be somewhat compensated for, by approximating the summation in (43) at $z=0$ using relevant Taylor series expansions for $ka \lesssim 1$ in the manner described in Appendix E. The summation in (43)

may then be approximately written as

$$\sum_{n=1}^{\infty} T_{0n}\, e^{-\gamma_{0n} z} = \begin{cases} \frac{1}{2}\,(1-\cos\theta_i) K_+(-k\cos\theta_i) \sum_{m=1}^{4} S_m(\theta_i)(ika)^m; & z=0 \\ \sum_{n=1}^{N} T_{0n}(\theta_i) e^{-\gamma_{0n} z} \quad ; \quad e^{-\gamma_{0n} z} << 1 \end{cases} \tag{47}$$

where

$$S_1(\theta_i) = 0.5831 \tag{48}$$

$$S_2(\theta_i) = -0.1364\ [\tfrac{1}{2} + \cos\theta_i] \tag{49}$$

$$S_3(\theta_i) = -0.0498\ [\tfrac{7}{8} - \tfrac{1}{2}\cos\theta_i - \cos^2\theta_i] \tag{50}$$

$$S_4(\theta_i) = 0.0198\ [\tfrac{9}{16} + \tfrac{11}{8}\cos\theta_i - \tfrac{1}{2}\cos^2\theta_i - \cos^3\theta_i] \tag{51}$$

which is sufficiently accurate for most engineering applications up to $ka \approx 1$.

6.2 Internal currents on a semi-infinite transmitting antenna

The current which penetrates into the end of a semi-infinite $(0 \le z \le \infty)$ cylindrical transmitting antenna having a delta function voltage source of strength, V_0 volts, at $z=z_0$ is associated with TM_{0n} circular waveguide modes and may be written in an analogous manner with respect to the receiving case as,

$$\{I^T_{s\infty}(z)\}_{int} = I^T_{\infty}(z_0;0)\left[-\frac{ik}{\pi} K_+(k)\right] \int_{\Gamma_1} \frac{K_+(-\alpha)e^{-i\alpha z}}{(k^2-\alpha^2)K(\alpha)}\, d\alpha \ ; \ 0 \le z \le \infty \tag{52}$$

where $I_{\infty}^{T}(z_0;0)$ is the incident current from (19) at the end. Again the contour, Γ_1, is given in Figure 1 and K_+ is the plus factor of $K(\alpha)$ in (4) discussed in Appendix C. The integral may be evaluated exactly by finding the residues of the poles of $[K(\alpha)]^{-1}$ enclosed by Γ_1 and (52) may then be approximated by,

$$\{I_{s\infty}^{T}(z)\}_{int} = V_0 U_s(z_0) \sum_{n=1}^{\infty} T_{0n}(\pi)\, e^{-\gamma_{0n} z} \tag{53}$$

where we have replaced the exact incident current, $I_{\infty}^{T}(z_0;0)$ with the approximate quantity, $V_0\, U_s(z_0)$ from (20). T_{0n} and γ_{0n} have been defined in (44) and (45), respectively. Again, as in the receiving formulation, we may approximate the summation in (53) with the expression in (47).

It should be noted that there would also be internal wall currents on the semi-infinite transmitting antenna which would not come from penetration at the cylinder end but rather would be excited directly by the source. For a delta function voltage source, this internal current can be shown to possess a logarithmic singularity at the feed-point similar to the logarithmic singularity of the external current at the input. For a more realistic excitation, such as a finite gap, however, the internal current would be well-behaved everywhere and would be directly related to a capacitive susceptance component (assuming there to be negligible radiation from the open end of the cylinder which in turn implies, $e^{-\gamma_{01} z_0} << 1$) of the overall input admittance. And since we have not addressed ourselves to the task of specifically defining a "realistic" input susceptance, the internal current in the vicinity of the voltage source and its effect on the input admittance will not be pursued any further in this report.

6.3 Internal current on a finite-length receiving antenna

From the external receiving current expression in (35), we may write the internal penetrating current near $z = -h$ using the transmission characterization in (43) as,

$$I^R_{int}(\theta_i;z) = E^i_\theta \sum_{n=1}^{\infty} \{V(\pi-\theta_i,+h)\ T_{0n}(\theta_i) + C^R(\pi-\theta_i)\ T_{0n}(\pi)\}\ e^{-\gamma_{0n}(h+z)} \quad ;\ z \approx -h \qquad (54)$$

while the penetrating current near the opposite end at $z = +h$ is obtained by replacing θ_i with $\pi-\theta_i$ and $(h+z)$ with $(h-z)$ in the above expression. The first term in the {brackets} above corresponds to TM_{0n} mode currents on the internal walls of the cylinder due to the primary current term, $E^i_\theta\ V(\pi-\theta_i;+h)$, while the second term corresponds to TM_{0n} mode currents due to the total external current incident upon $z = -h$ arising from reflections eminating from the opposite end at $z = +h$. These latter currents are analogous to waves incident at an angle, $\theta_i = \pi$. Hence, the transmission coefficient for these incident currents is evaluated at $\theta_i = \pi$. The expression in (47) may be used to approximate the summations in (54), thereby reducing the computational efforts required to find the internally penetrating current. Note, it is implicit in this formulation, that there is no internal interaction between the ends of the cylinder, thus implying that $e^{-\gamma_{01}2h} << 1$.

6.4 Internal current on a finite-length transmitting antenna

The internal penetrating current near the ends of a finite length $(-h \le z \le h)$ cylindrical transmitting antenna may be obtained by applying the transmission characterization in (53) to the respective incident currents from (38) with the result,

$$I^{T}_{int}(z \approx \mp h) = V_0 \{U_s(h \pm z_0) + C^{T}(h \pm z_0)\}$$

$$\sum_{n=1}^{\infty} T_{0n}(\pi)\, e^{-\gamma_{0n}(h \pm z)} \qquad (55)$$

Analogous to the receiving case, the first term in (55) corresponds to TM_{0n} mode currents on the internal walls of the cylinder due to the primary current, $V_0\, U_s(|z - z_0|)$ at $z = \mp h$ while the second term corresponds to TM_{0n} mode currents due to the total external current incident upon $z = \mp h$ arising from reflections eminating from the opposite end. Again, (47) may be used to approximate the summations in (55) and the restriction, $e^{-\gamma_{01}(h \pm z_0)} << 1$, is also implied in this formulation.

6.5 End conductance of a finite length cylindrical antenna

A quantity related to the internally penetrating current on a cylindrical antenna is the input conductance for a TM_{0n} mode incident upon one of the ends of the antenna. Unlike the cases treated by Weinstein [2, Chap. 1], Levin and Schwinger [23], Jones [24] and others, our analysis for the end conductance, discussed in Appendix F, deals with a TM_{0n} mode under cut-off, the radiation in this case necessarily coming from tunneling. The end conductance in this situation is relevant and very important to EMC studies involving the penetration into the end of a cylindrical enclosure [25]. A detailed discussion of this quantity is left to Appendix F, where the end conductance as seen by an evanescent TM_{0n} mode inside and near the end of a finite length cylinder based upon Wiener-Hopf analyses and the multiple reflection concept is derived.

Section 7 Numerical results for the finite length cylindrical antenna

Due to the restriction our theory places upon the electrical radius of $ka \lesssim 1$, the currents on the internal wall of the finite length cylindrical receiving or transmitting antenna are, in general, very much smaller in magnitude than the currents on the external wall, except in the near vicinities of the ends. From Section 6, it may be ascertained, that the internal current is significant only within a distance, $2a$, (equal to one cylinder diameter) from either end. And since we cannot rely upon results from our external current expressions so close to the ends, where the internal currents are significant, the formation of total current distributions from the combinations of our receiving and transmitting external current distributions in (35) and (38), respectively, with the corresponding internal current distributions in (54) and (55) would be of little advantage. Hence, in most cases, the external current formulas in (35) and (38) will be sufficient to describe the current distribution, whether it be the total or external only, on finite length receiving or transmitting antennas, respectively. On the other hand, the internal current distributions given in (54) and (55) for the finite length receiving and transmitting cylindrical antennas may be accurately calculated using the approximate formula in (47) at practically any point on the antenna.

7.1 Current distribution on a receiving antenna

In order to examine differences in our receiving theory resulting from the use of either approximate form of $U(\theta_i;z)$ in (9) or (13) we have included Figure 17 which shows the magnitude of the induced current at the center of a receiving antenna where $\Omega(h) = 10$, illuminated by

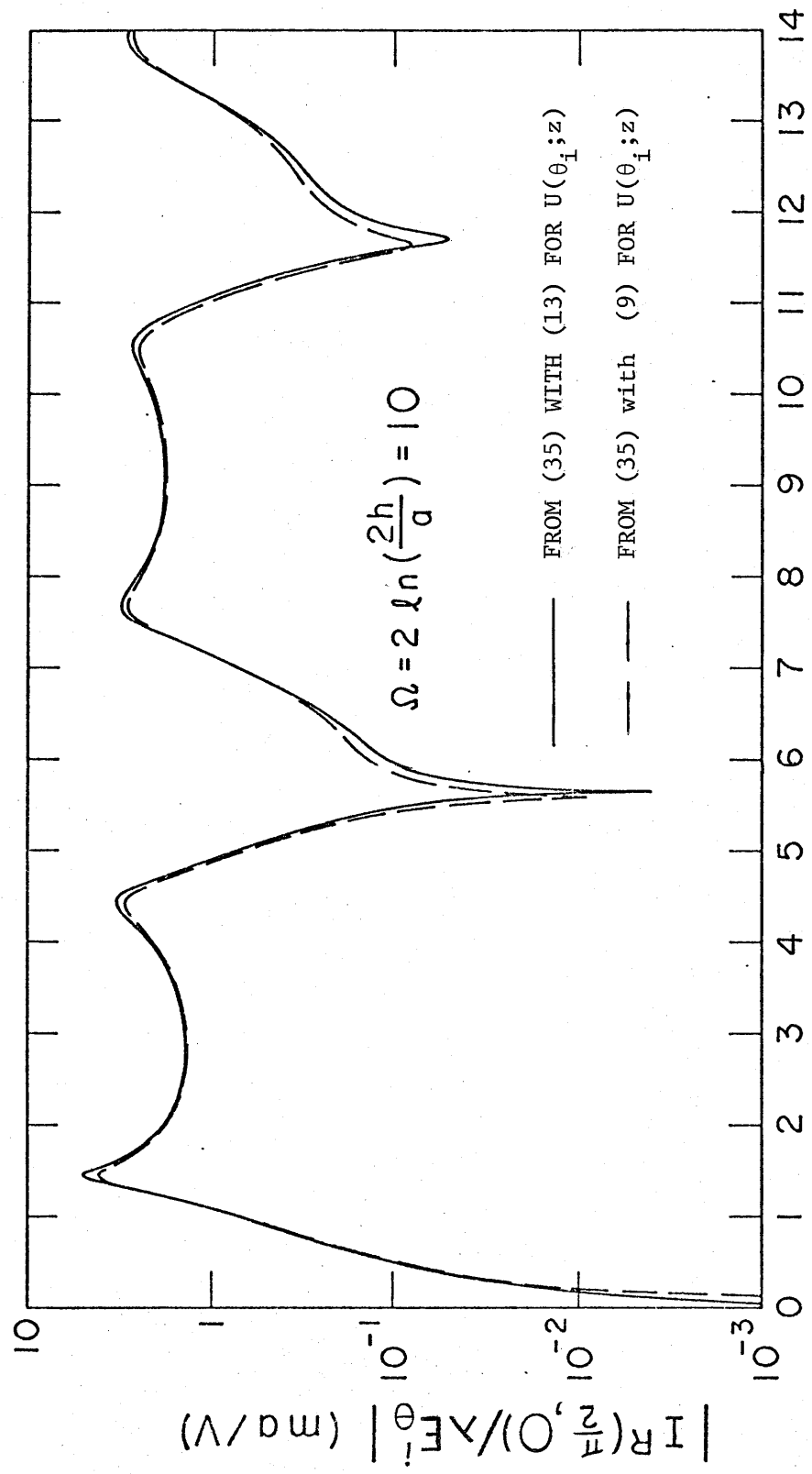

Figure 17. Magnitude of the current at the center of a cylindrical receiving antenna due to a normally incident uniform plane wave as a function of the electrical half-length, kh, and normalized to the incident electric field and the wavelength.

a normally incident ($\theta_i = \pi/2$) plane wave polarized parallel to the antenna as a function of the electrical length, using both (9) and (13) in the finite length receiving antenna current expression in (35). As expected, the agreement between both results is very good except near resonances and anti-resonances. And comparisons with existing analytical and numerical results for cylindrical antennas in which the condition, $\Omega(h) >> |\ell n(v_0)|$ in (8), is satisfied, have indicated that our theory yields slightly better results in almost every case when (13) is used for $U(\theta_i; z)$. For these reasons, in what follows we shall present only results obtained from the use of (13) for $U(\theta_i; z)$ in the receiving and transmitting expressions in (35) and (38), respectively.

The current distributions on a half-wave, $kh = \pi/2$, receiving antenna where $\Omega(h) = 2\,\ell n(2h/a) = 10$ for the incident angles, $\theta_i = \pi/36, \pi/6, \pi/3$ and $\pi/2$ as calculated from (35) are shown in Figure 18. For comparison, first order results from the King-Middleton theory [11, Chap. IV, Sec. 7] and results from King's three term theory [5] for the normal incidence case, $\theta_i = \pi/2$, are also shown. The agreement between the latter King theory and ours in this particular case is excellent. And the overall agreement between all theories is quite acceptable. We note that in spite of the condition in (8) which requires $\Omega(h) = 2\,\ell n(2h/a) >> |\ell n(v_0)|$, the current distribution predicted by our formulas in the near-grazing situation, $\theta_i = \pi/36$, is at a physically anticipated small level. This is further exemplified in Figure 19, where for the same antenna as in Figure 18 the currents at $z = 0$, $h/3$ and $2h/3$ are illustrated as a function of the incident angle, θ_i. And we note the near sinusoidal variation of the current with respect to the incident angle, θ_i, as would be expected for a thin half-wave dipole.

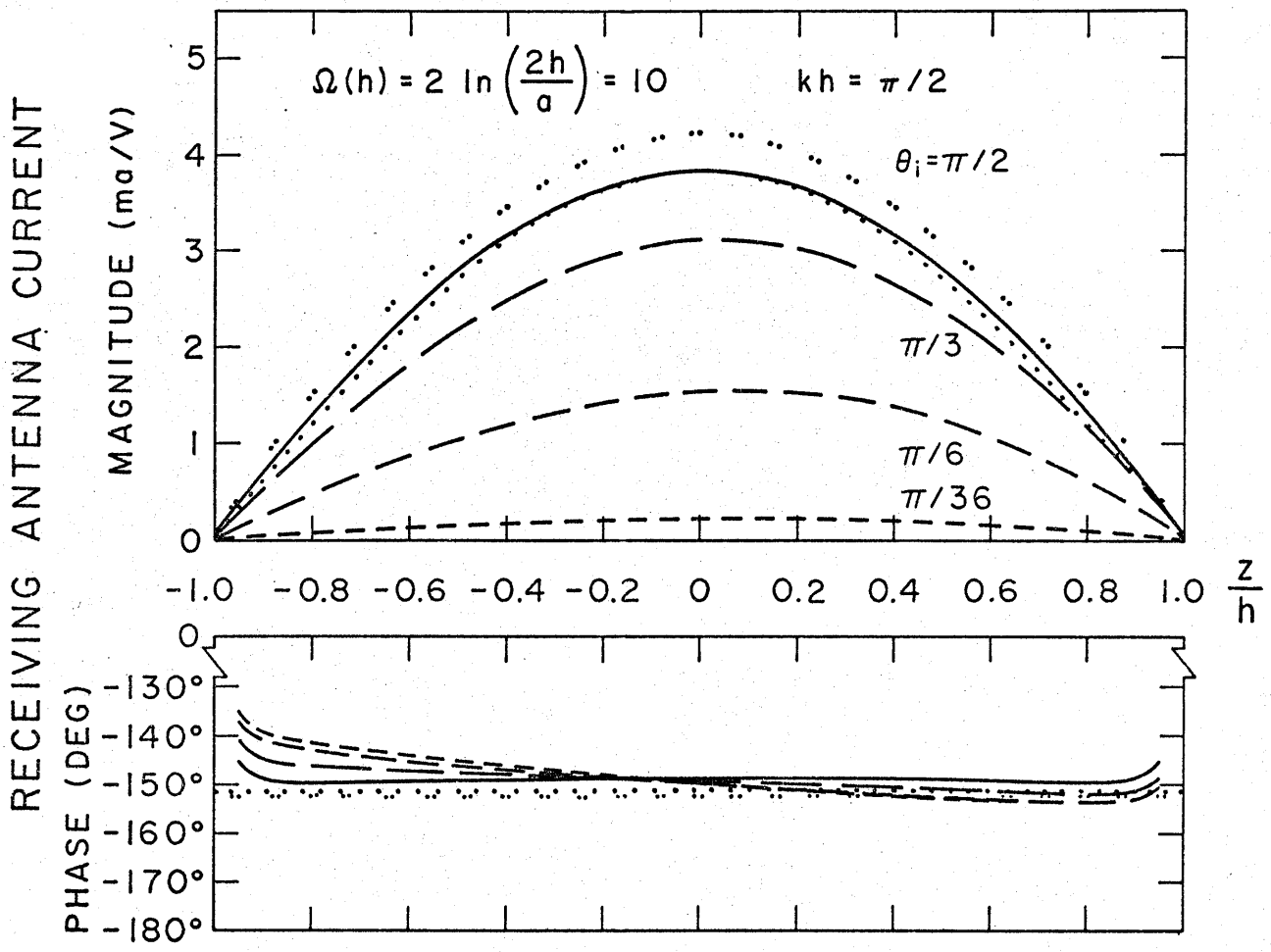

Figure 18. Current distribution on a thin half-wave receiving antenna normalized to the incident electric field and the wavelength, i.e., $I^R(\theta_i;z)/\lambda E^i_\theta$.

——————— $\theta_i = \pi/2$
— — — — $= \pi/3$
— — — — — $= \pi/6$
— — — — — $= \pi/36$
} from eq. (35) with (13) used for $U(\theta_i;z)$

. . . . . $\theta_i = \pi/2$ Three term theory of King [5]

.. .. $\theta_i = \pi/2$ First order King-Middleton theory [II, Sec. IV.7]

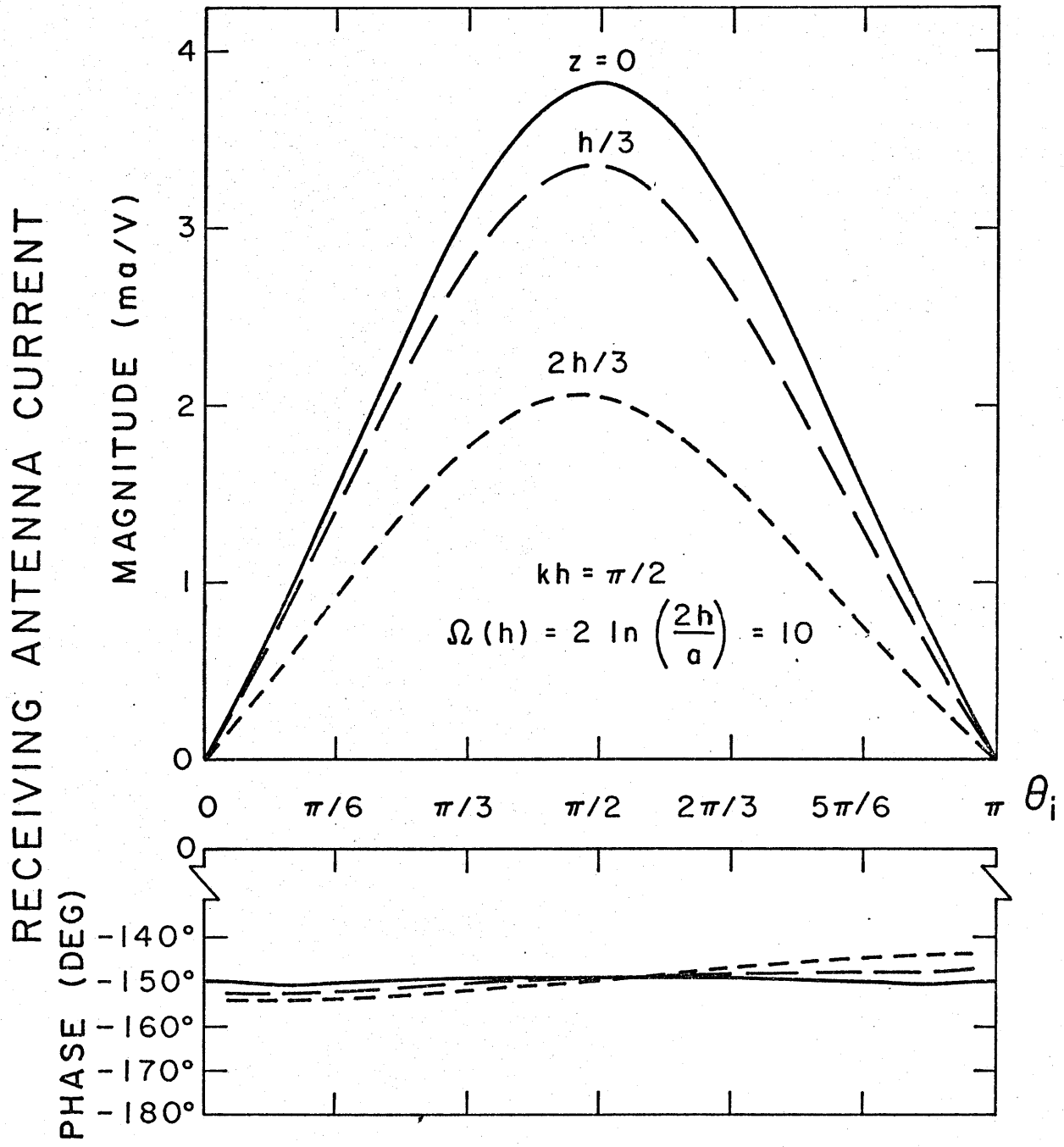

Figure 19. Current at specific positions on a thin half-wave receiving antenna as a function of the incident angle, θ_i, calculated from eq. (35) with (13) used for $U(\theta_i;z)$, and normalized to the incident electric field and the wavelength, i.e., $I^R(\theta_i;z)/\lambda E^i_\theta$.

The currents on the internal walls of the same receiving antenna ($kh = \pi/2$, $\Omega(h) = 10$) at the end, $z = -h$, and slightly away from the end, $z = -h + 2a$, as calculated from (54) with (47) are shown in Figure 20 as a function of the incident angle, θ_i. The internal current at the end, $z = -h$, represents an infinite summation of all the TM_{0n} mode currents at this point and is equal in theory to the negative of the external current at this end. While the internal current at $z = -h + 2a$ is predominantly associated with the TM_{01} circular waveguide mode, all the higher order modes being much more attenuated at this point. Thus beyond $z = -h + 2a$, the internal current will decay essentially as $e^{-\gamma_{01}(h+z)}$.

The current distribution on an electrically thick ($ka = 1.0$) receiving antenna three wavelengths in length as calculated from (35) is shown in Figure 21 for the incident angles, $\theta_i = \pi/36, \pi/6, \pi/3$, and $\pi/2$. Note that this distribution corresponds only to the external azimuthally uniform z-directed current on the cylinder. Note also that since $\Omega(h) = 2\,\ell n(2h/a) = 5.87$ and $|\ell n(v_0)| = 2.64$, 0.93, 2.24, and 3.63 for the respective angles considered, the condition that $\Omega(h) >> |\ell n(v_0)|$ as originally required in the analytical development, no longer holds. However, the correspondence with the data from Wu, et al., [35] based upon the integral equation and product integration formulation of Kao [18] for the azimuthally uniform z-directed current also shown in Figure 21 for the same antenna with a normally incident plane wave is surprisingly good. Again we bring attention to the relatively small level of current on the antenna predicted by our theory at near-grazing incidence, $\theta_i = \pi/36$. The behavior of the current at $z = 0$, $h/3$ and $2h/3$ with respect to the incident angle, θ_i, is shown in Figure 21 and

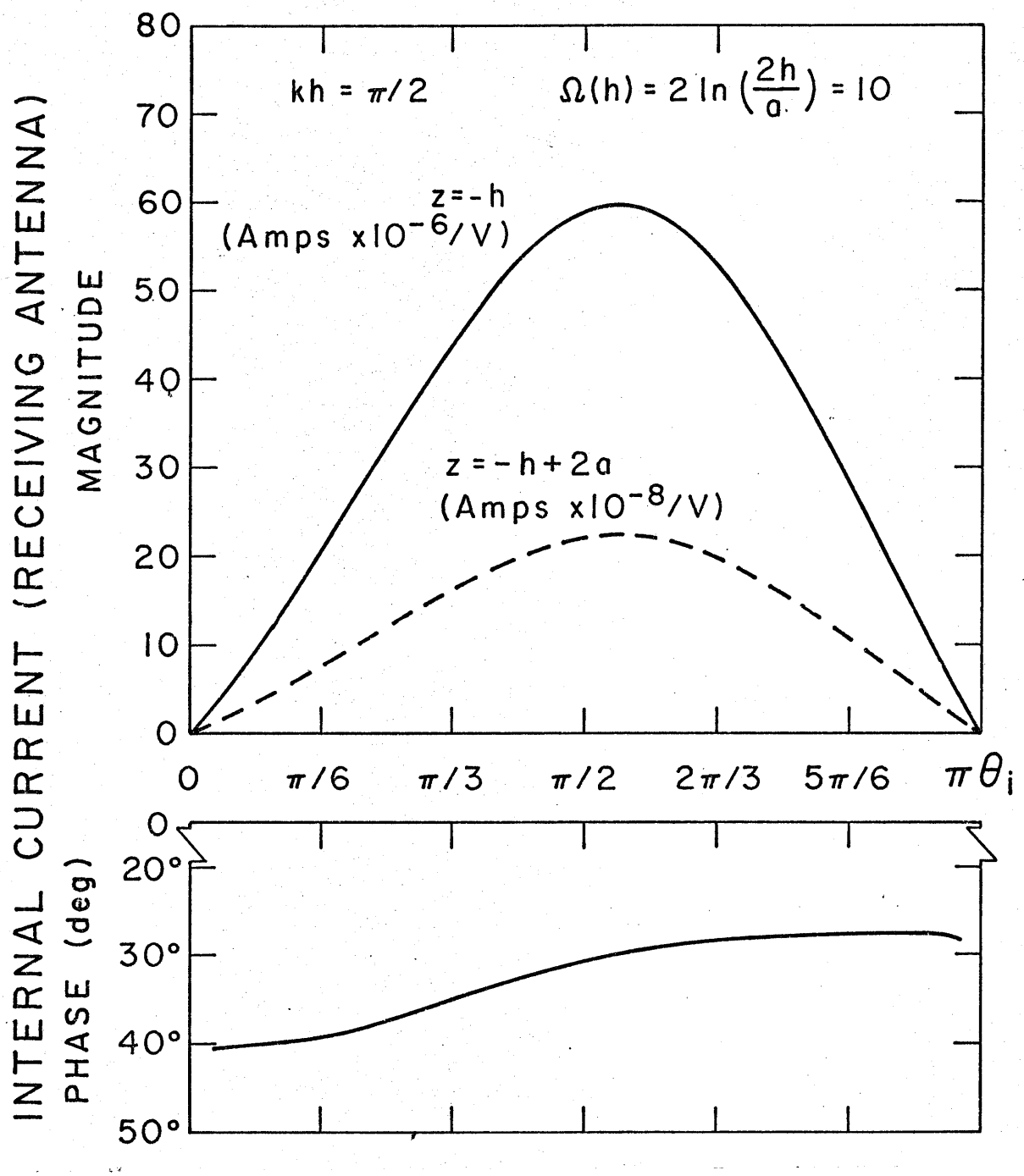

Figure 20. Internal current at the end and slightly within the end of a thin half-wave receiving antenna as a function of the incident angle, θ_i, calculated from eq. (35) with (13) used for $U(\theta_i;z)$, and normalized to the incident electric field and the wavelength, i.e., $I^R_{int}(\theta_i;z)/\lambda E^i$.

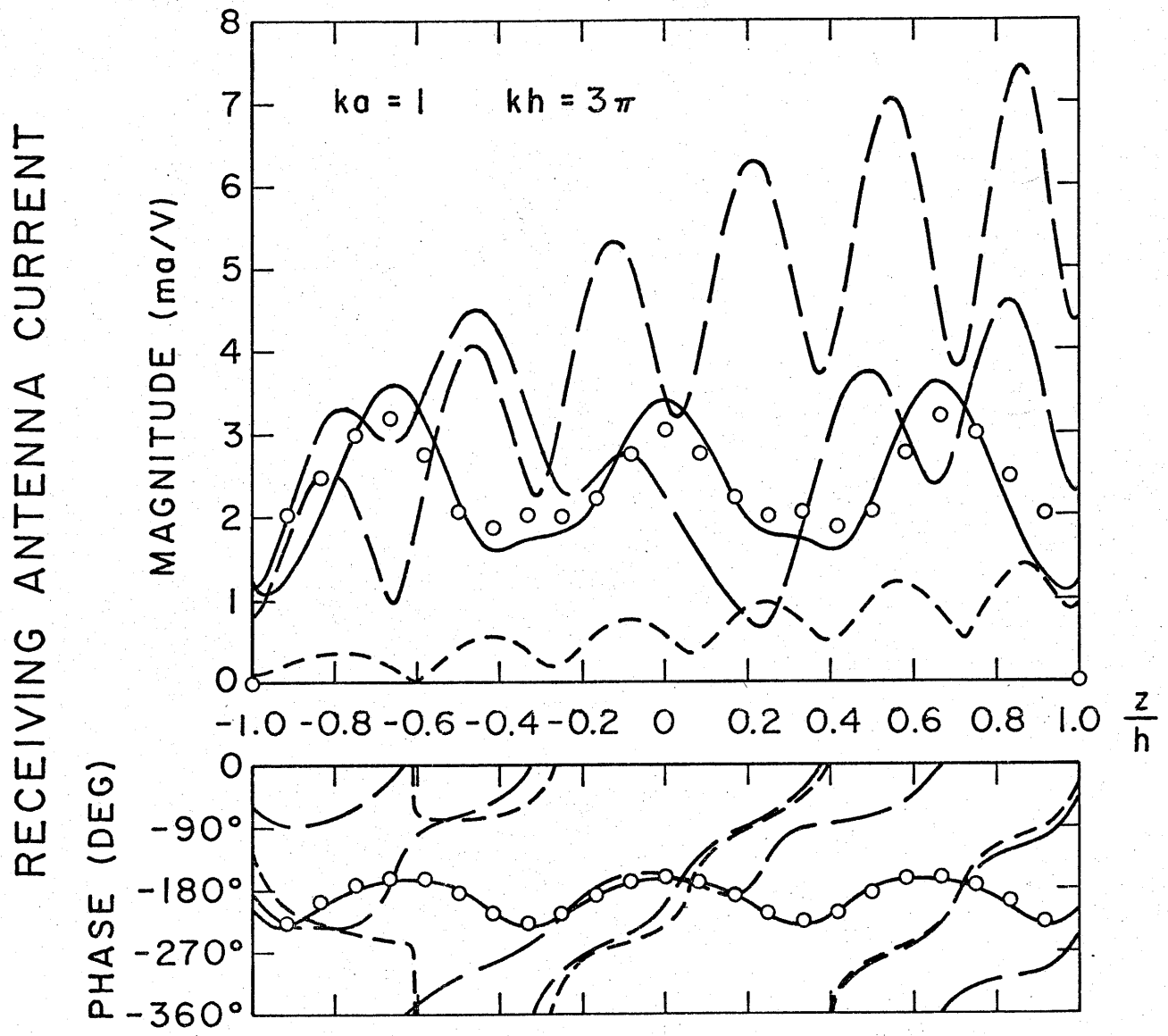

Figure 21. Current distribution on a three wavelengths long, electrically thick, receiving antenna normalized to the incident electric field and the wavelength, i.e., $I^R(\theta_i;z)/\lambda E^i_\theta$.

——————— $\theta_i = \pi/2$
— — — — — $= \pi/6$
— — — — — $= \pi/3$
— — — — — — $= \pi/36$

} from eq. (35) with (13) used for $U(\theta_i;z)$

o $\theta_i = \pi/2$ Numerically evaluated data from Wu, et al. [35]

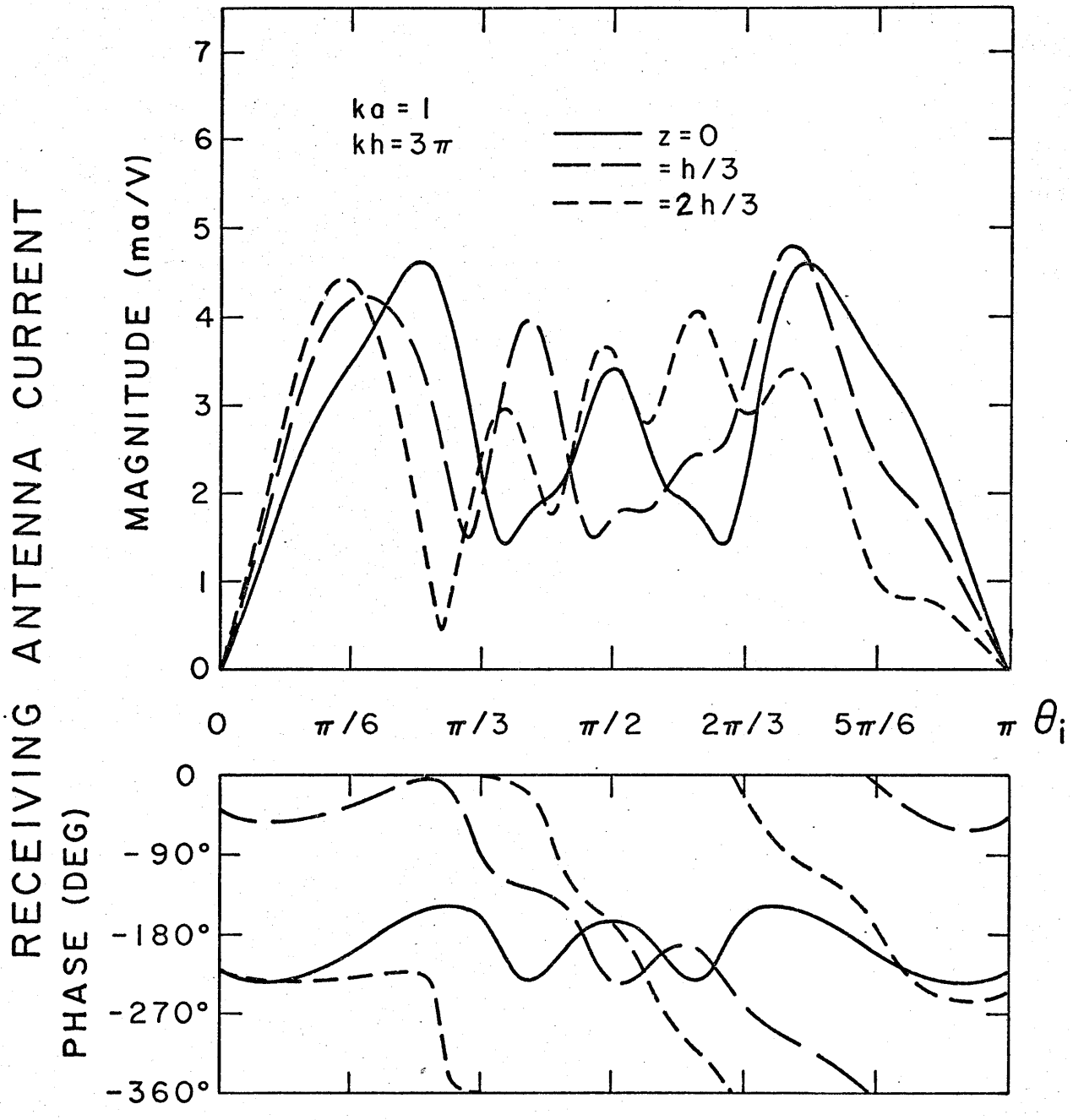

Figure 22. Current at specific positions on an electrically thick receiving antenna as a function of the incident angle, θ_i, calculated from eq. (35) with (13) used for $U(\theta_i;z)$, and normalized to the incident electric field and the wavelength, i.e., $I^R(\theta_i;z)/\lambda E^i_\theta$.

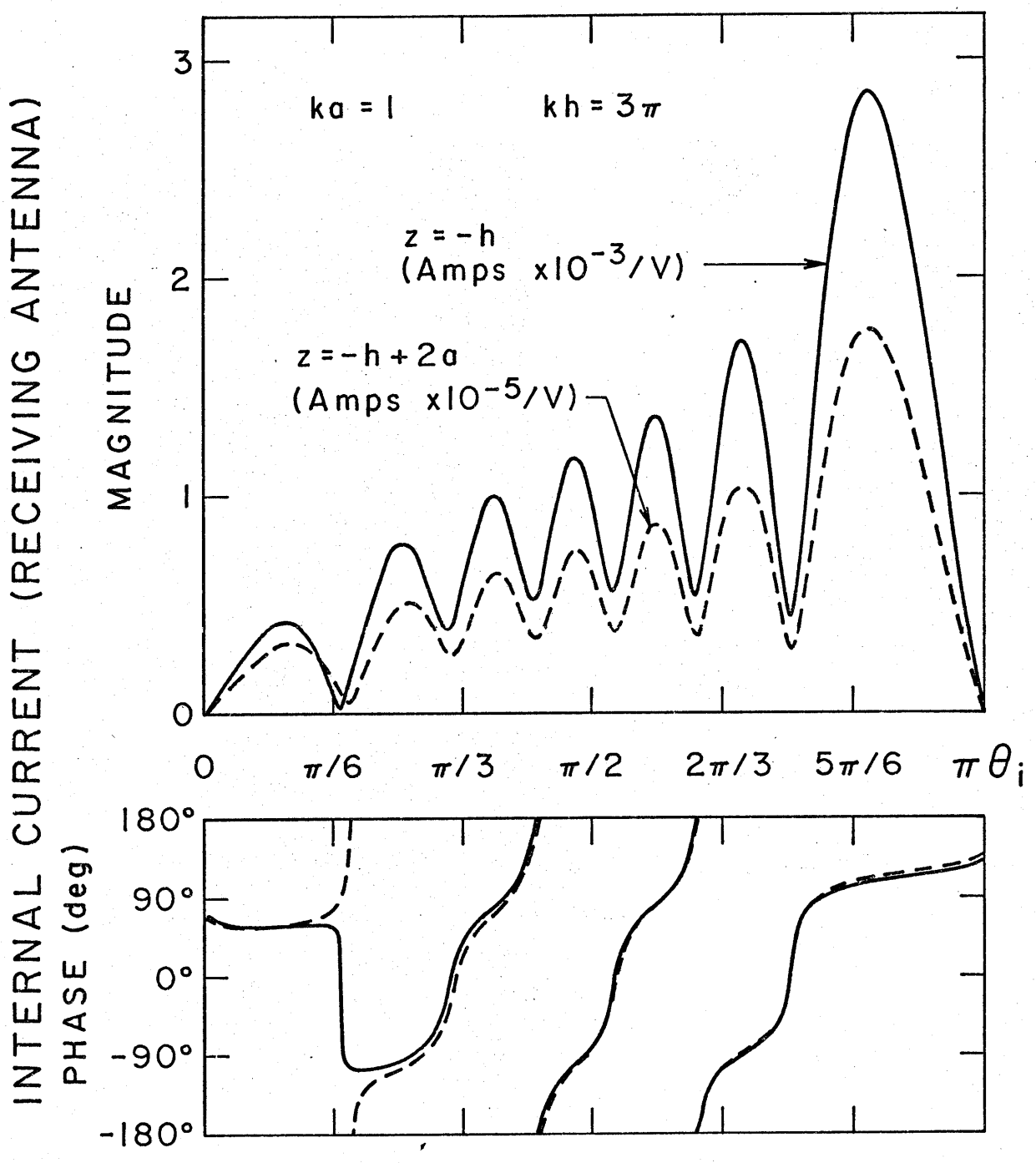

Figure 23. Internal current at the end and slightly within the end on an electrically thick receiving antenna as a function of the incident angle, θ_i, of the uniform plane wave, calculated from eq. (35) with (13) used for $U(\theta_i;z)$, and normalized to the incident electric field and the wavelength, i.e., $I^R_{int}(\theta_i;z)/\lambda E^i_\theta$.

is seen to exhibit the physically expected result of zero current at grazing incidence, $\theta_i = 0$ and π. The currents on the internal walls of this receiving antenna ($kh = 3\pi$, $ka = 1$) at the end, $z = -h$, and slightly away from the end, $z = -h + 2a$, as calculated from (54) with (47) are shown in Figure 23 as a function of the incident angle, θ_i. Comments similar to the ones given for the internal currents illustrated in Figure 20 are also applicable to this much thicker and longer antenna.

7.2 Current distribution on a transmitting antenna

As discussed at the beginning of this section, the total (internal + external) current distribution on those cylindrical antennas (both transmitting and receiving) for which out theory is applicable is for all practical purposes given by the external current distribution alone, except in the near vicinity of the ends. An additional exception to this, which is particular to the transmitting antenna, is the region very close to the source where internal currents are directly excited by the source, itself. A brief disucssion of this localized internal current has already been given in Section 6.4, where it was deemed inappropriate to pursue an in depth study of this current, which is of secondary importance.

The current distribution on a center-driven half-wave antenna where $\Omega(h) = 2\ \ell n(2h/a) = 10$ as calculated from (38) is shown in Figure 24 along with corresponding data from the three-term theory of King [5] and the approximate second order iteration procedure of King and Middleton [11, Chap. II, Sec. 22]. The agreement between our results and the latter theory with regard to the real component of the current is excellent. And although the agreement between the imaginary components is acceptable, the discrepancy here was not totally unexpected since in the process of

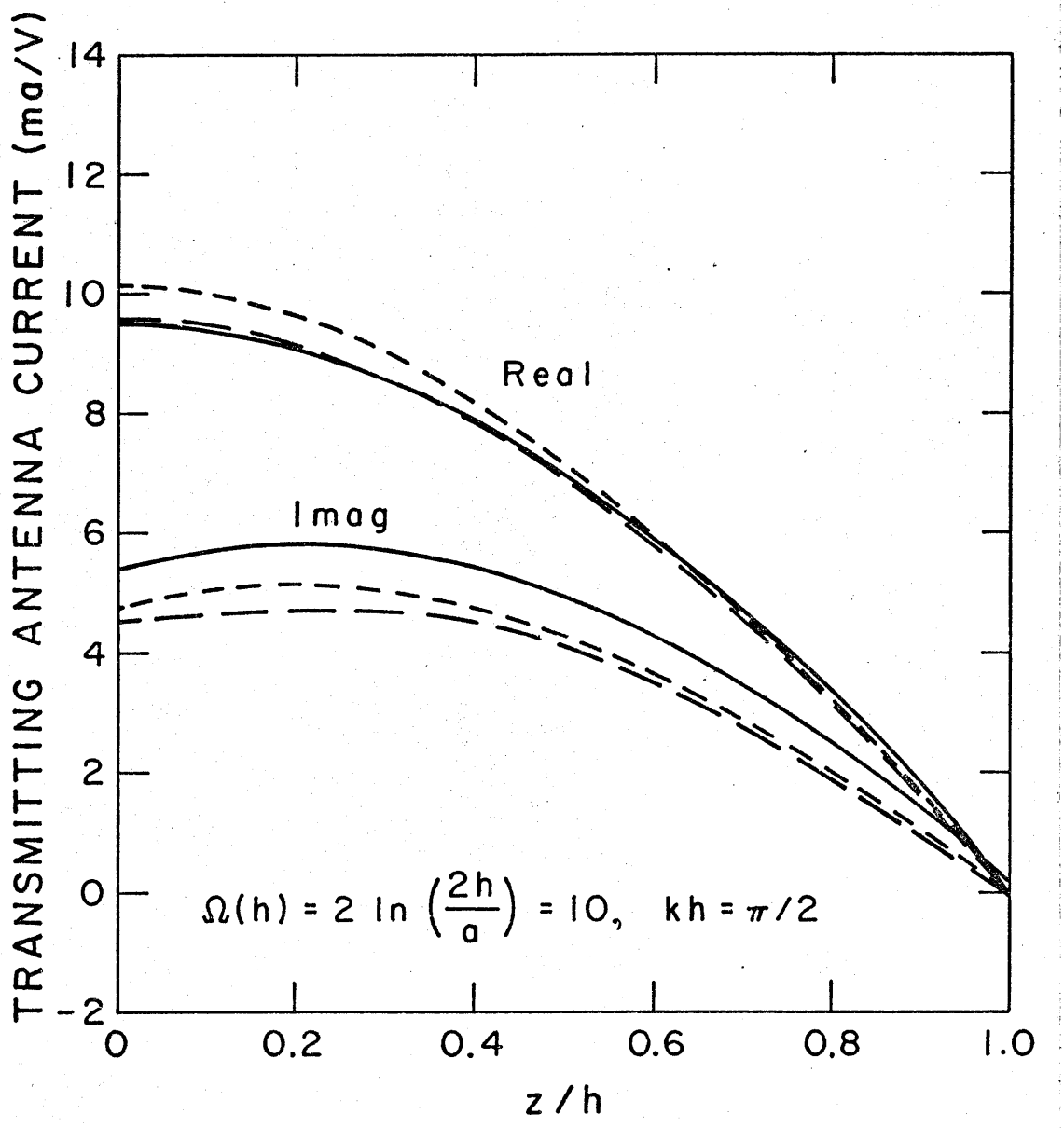

Figure 24. Current distribution on a thin, center fed, half wave transmitting antenna.

———— from eq. (38) with (13) used for $U(\pi;z)$.

—— —— approximate second order King-Middleton theory [11, Chap. II, Sec. 22]

— — — — King three-term theory [5]

achieving an accurate value for the real component of the primary current discussed in Section 3.2, a less accurate "physically acceptable" value of the imaginary current near the source resulted. The correspondence between the three-term theory of King (which may be judged to be less accurate [5] than the King-Middleton results) and our theory is also quite acceptable.

Perhaps more important than the transmitting current distribution, is the input admittance to the antenna. Therefore, in Figures 25 and 26 we show the input conductance and susceptance, respectively, as calculated from (41) for a center-driven cylindrical antenna where $\Omega(h) = 2\ \ell n(2h/a) = 10$, as a function of the electrical length, kh. Corresponding admittance data from the three-term theory of King [5] and second order results from the iterative method of King and Middleton [11, Chap. II, Sec. 30] are also shown in these figures. The agreement between the conductances predicted by all three theories in Figure 25 is seen to be very good. The agreement between the input susceptances is also very good for the smaller values of kh where the "realistic" imaginary component of the primary current is small compared to imaginary current arising from the multiple reflections from the ends. At the larger values of kh, where ka is proportionally larger, we find larger discrepancies between our results and the King three term and King-Middleton results. Here the imaginary component of the primary current significantly affects the overall input susceptance. And since our approximate expression for the primary transmitting current in (20) is not expected to accurately estimate the "realistic" value for the imaginary input current, this discrepancy will also appear in the finite length antenna susceptance calculated from (41) in which (20) is used.

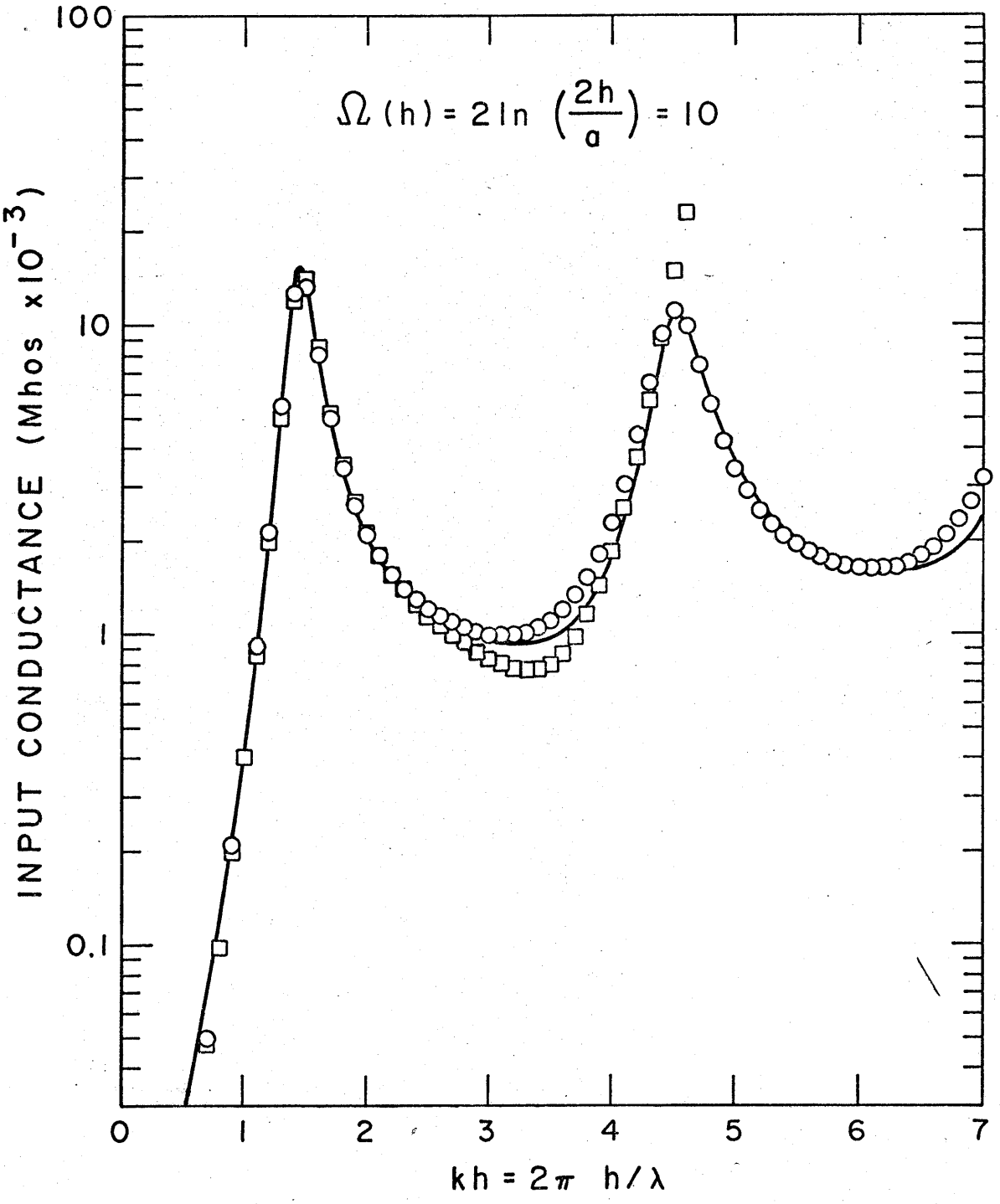

Figure 25. Input conductance of a thin center fed cylindrical antenna.

——— from eq. (41) with (13) used for $U(\pi;z)$

○ Second order King-Middleton theory [11, Chap. II, Sec. 30]

□ King three-term theory [5]

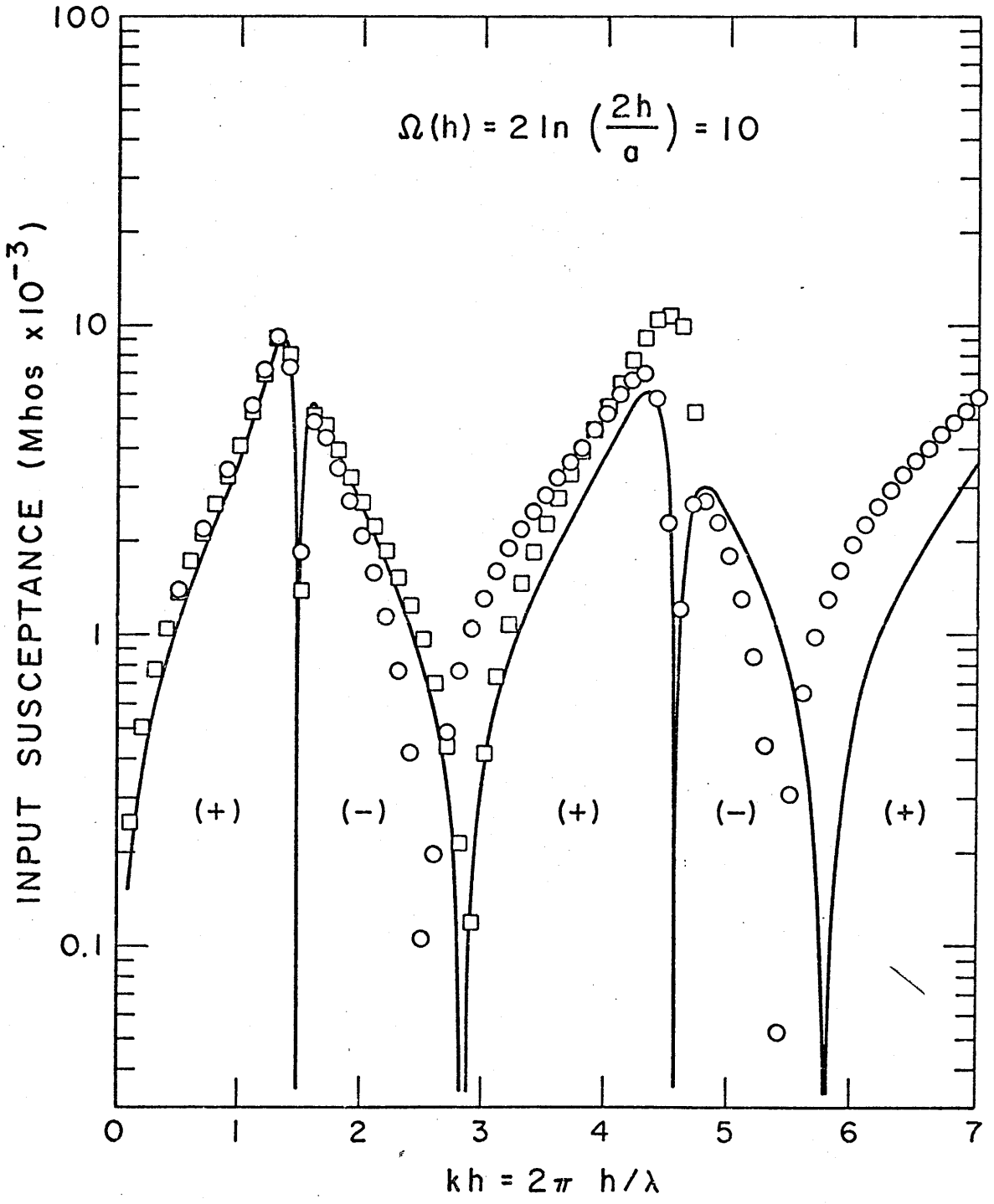

Figure 26. Input susceptance of a thin center fed cylindrical antenna.

———— from eq. (41) with (13) used for $U(\pi;z)$

○ Second order King-Middleton theory [11, Chap. II, Sec.30]

□ King three-term theory [5]

However, in practical situations the input susceptance may be eliminated by appropriate matching leaving the input conductance essentially unchanged and the most important quantity of consideration.

To provide further comparison of our theory with existing approaches we offer Figure 27 which shows the input conductance to a center-driven cylindrical antenna where the ratio of antenna half-length to radius is $h/a = 100$ as calculated by (41) and the corresponding numerically evaluated (via the moment method) results of Harrington and Mautz [26]. The agreement between our results and the accurate numerically-determined data is excellent. Further evidence to substantiate our theory is given in Figure 28, which is the same as the previous figure except the driving point is now located at $z = \pm h/2$. Excellent correspondence with the numerically determined data of Harrington and Mautz [26] is once more attained.

We extend our considerations to much thicker antennas with Figure 29, which shows the input conductance of cylindrical antennas as calculated from (41) for the radii normalized to wavelength, $a/\lambda = 0.0159$, 0.078, and 0.164 ($ka = 0.1$, 0.49 and 1.03 , respectively) as a function of the normalized half-length, h/λ , between 0.1 and 0.5 . And although these antennas are out of the applicable range of our theory due to the basic condition in (8), we find behavior still consistent with the numerically-obtained results of Chang [27] and [28] (one-sided delta function excitation data), and the experimental results of Hartig [29]. This further enhances the feeling that the derived result actually has a much wider application than had been assumed analytically. And we note the very good agreement between our theory and the others for the larger values of h/λ , where the ratio of h/a is also larger.

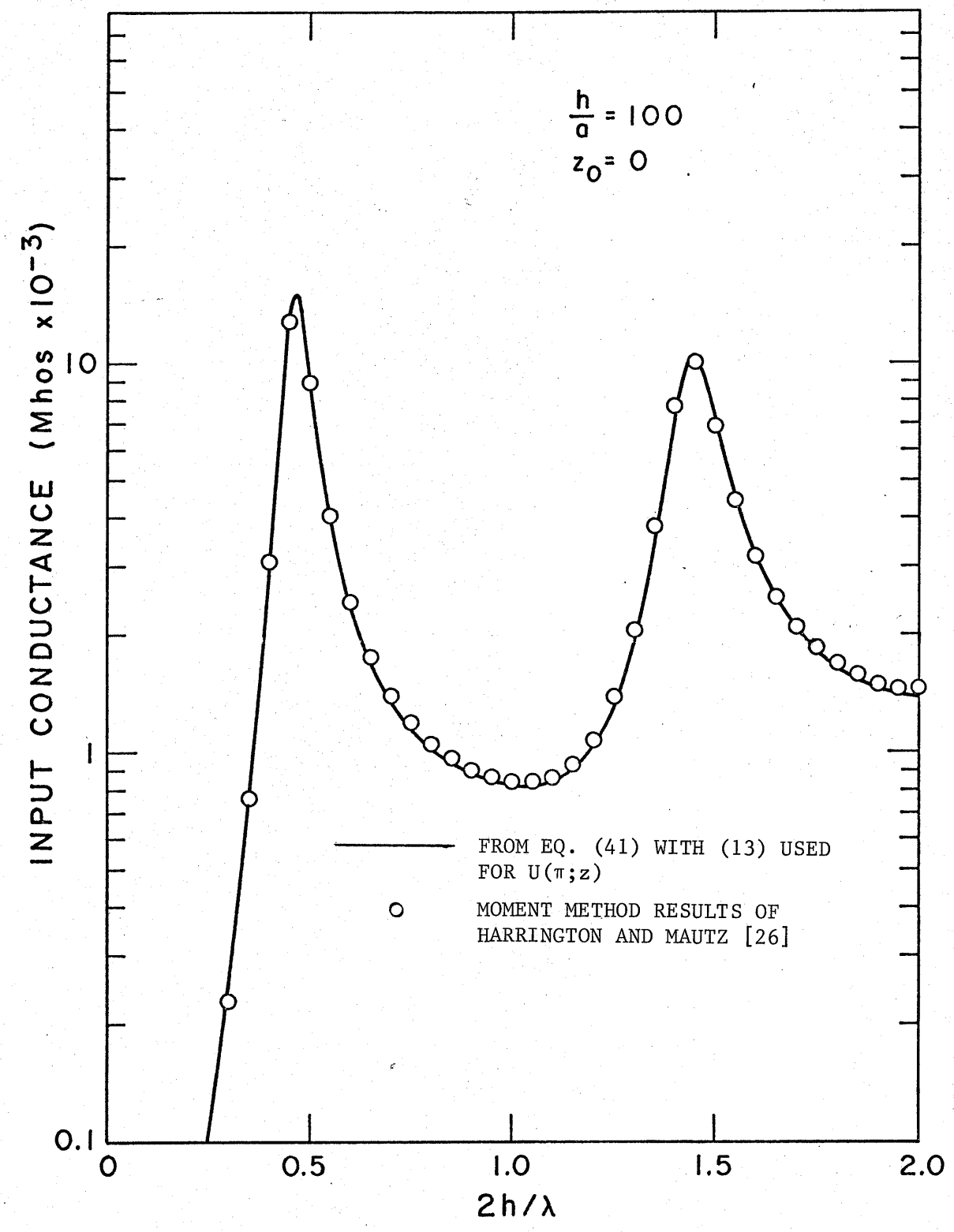

Figure 27. Input conductance of a center fed cylindrical antenna as a function of the normalized length, $2h/\lambda$.